ACCSCIENCE PUBLISHING

International Journal of Bioprinting

REVIEW ARTICLE

Scaling liver bioprinting: A guide for usage of the hepatic extracellular matrix as a bioink

Valentin A. Brumberg[1], Polina Yu. Bikmulina[1]*, Artem A. Pozdnyakov[1], Zahra Heydari[1], Darya R. Zimulkina[1], Olga A. Smirnova[1], Frederico David Alencar de Sena Pereira[1], Anastasiia M. Nesterova[1], Svetlana L. Kotova[1], Massoud Vosough[2,3], Anastasia I. Shpichka[1], and Peter S. Timashev[1,4,5]*

[1]Institute for Regenerative Medicine, Sechenov University, Moscow, Russia

[2]Department of Regenerative Medicine, Cell Science Research Center, Royan Institute for Stem Cell Biology and Technology, ACECR, Tehran, Iran

[3]Experimental Cancer Medicine Group, Institution for Laboratory Medicine, Karolinska Institute, Stockholm, Sweden

[4]World-Class Research Center "Digital biodesign Biodesign and Personalized Healthcare", Sechenov University, Moscow, Russia

[5]Chemistry Department, Lomonosov Moscow State University, Moscow, Russia

(This article belongs to the Special Issue: *Made-to-order Organ*)

Abstract

Hydrogels derived from the decellularized extracellular matrix (dECM) are widely used in three-dimensional (3D) bioprinting, mainly because they recapitulate the native tissue microenvironment and retain key growth factors and cytokines. Hence, they are characterized by adequate biocompatibility for use in 3D bioprinting. In liver tissue engineering, these materials, along with liver-derived cell types, can serve as appropriate *in vitro* hepatic models for drug efficiency testing and liver metabolism studies. These hydrogels can also be considered as good manufacturing practice-compliant systems for liver cell and organoid expansion, unlike routinely used basal membrane extract products derived from tumorigenic cell lines. Although weak mechanical properties and poor printability hinder the direct usage of dECM hydrogels as bioinks, various modifications of dECM and the bioprinting process are applied to overcome these problems. However, there are several complications regarding the scale-up and good laboratory practice-compliant manufacturing of these hydrogels: (i) the manufacturing standards for dECM hydrogels are not well established; (ii) the methods for obtaining these hydrogels are slightly varying, resulting in decreased reproducibility; and (iii) since these hydrogels are traditionally produced from animal tissue, the animal-to-animal variability, different harvesting conditions, and bioburden reduction need to be thoroughly considered. This review examines the essential properties of dECM hydrogels for biomedical applications, focusing on biocompatibility, mechanical strength, and bioactivity. Additionally, this review discusses production methods and modifications for 3D bioprinting, highlights case studies of dECM-based liver constructs, and addresses challenges in scalability and regulatory hurdles for clinical translation.

Keywords: Bioprinting; Decellularized extracellular matrix; Hydrogels; Liver biofabrication; Crosslinking; Photopolymerization; Large-scale manufacturing

***Corresponding author:**
Peter S. Timashev
(timashev_p_s@staff.sechenov.ru)

Citation: Brumberg VA, Bikmulina PY, Pozdnyakov AA, et al. Scaling liver bioprinting: A guide for usage of the hepatic extracellular matrix as a bioink. *Int J Bioprint*. 2025;11(1):57-83. doi: 10.36922/ijb.4343

Received: July 26, 2024
Revised: September 19, 2024
Accepted: September 26, 2024
Published Online: September 26, 2024

Copyright: © 2024 Author(s). This is an Open Access article distributed under the terms of the Creative Commons Attribution License, permitting distribution, and reproduction in any medium, provided the original work is properly cited.

Publisher's Note: AccScience Publishing remains neutral with regard to jurisdictional claims in published maps and institutional affiliations.

1. Introduction

Hydrogels can be defined as highly hydrated polymeric materials (with a water content of more than 30% of the wet weight), the structure of which is maintained by physical and/or chemical crosslinking of polymer chains. These three-dimensional (3D) networks of hydrophilic polymers undergo a phase transition (volume phase transition or sol–gel transition) under certain physical or chemical stimuli.[1] The polymers may be synthetic (polyethylene oxide, polyvinyl alcohol, polyacrylic acid, poly[propylene fumarate-co-ethylene glycol], etc.), natural (alginate, chitosan, collagen, hyaluronic acid [HA], etc.), or combined. Hydrogels of all origins are actively used as systems for drug and cell delivery to stimulate regenerative processes.

Natural hydrogels may be based upon a specific component (alginate, fibrin, chitosan, etc.) or composite mixtures of the extracellular matrix (ECM) components (e.g., a hydrogel of pig small intestine submucosa [SIS]). Hydrogels derived from decellularized ECM (dECM) stand out among natural hydrogels. These hydrogels are generally obtained by enzymatic hydrolysis, with crosslinking occurring at a physiological temperature and pH.[2] Unlike other hydrogels, which are represented by a single ECM component, these materials can reproduce the native microenvironment of cells. The ECM is known to be one of the universal components of the stem cell niche, along with the supporting cells and autocrine and paracrine factors.[3]

This review examines the essential properties that dECM hydrogels must retain to ensure their efficacy in biomedical applications. We begin by outlining the critical characteristics that are necessary for optimal functionality, including biocompatibility, mechanical strength, and bioactivity. Next, we delve into the various production methods for dECM, highlighting both conventional techniques and innovative modifications that enhance the material's performance. We explore strategies for modifying and crosslinking these hydrogels to improve their suitability for 3D bioprinting applications, emphasizing the importance of achieving the right balance between viscosity and printability. In addition, we provide a detailed analysis of different bioprinting approaches, discussing the unique features and advantages of each method. This section includes case studies and exemplary models of bioprinted dECM-based liver constructs, showcasing the potential of these technologies in tissue engineering and regenerative medicine. Finally, we address the challenges associated with large-scale manufacturing of dECM hydrogels, including scalability, reproducibility, and cost-effectiveness. We also consider the clinical translation of dECM-based products, discussing regulatory hurdles and the need for rigorous testing to ensure safety and efficacy in human applications. Through this review, we aim to highlight both the potential and complexities of utilizing dECM hydrogels in advanced biomedical applications.

2. Desired properties of liver dECM for bioink applications

2.1. Mechanical and structural properties

Stiffness is a key factor influencing cell behavior, impacting various cell functions like signaling, proliferation, differentiation, and metabolic activity. The normal liver has an average stiffness of approximately 1.5–2 kPa. However, healthy liver stiffness is reported in the literature to be within a wide range between 150 Pa and 6 kPa due to different measurement techniques. For example, the lowest stiffness value of 150 Pa was produced by indentation using atomic force microscopy, while 6 kPa was measured by the non-invasive FibroScan® method utilized in the clinic.[4,5]

It has been revealed that the porosity and pore sizes have a significant influence on the regeneration and function of cells. Introducing a more complex construct geometry with pores via bioprinting enhanced cell metabolic activity and spheroid sprouting.[6] Additionally, angiogenesis can be affected by the scaffold pore size and porosity, which may be designed in different ranges.[7] Numerous studies have suggested that an ideal scaffold requires an interconnected pore structure with high porosity to ensure adequate diffusion of nutrients for cells and waste products within the scaffold. Using different protocols to obtain dECM scaffolds and hydrogels, various pore sizes and porosity can be achieved.[4–8] Mao et al.[9] developed a bioink by combining methacrylated gelatin (GelMA) with dECM to encapsulate human-induced hepatocytes (hiHep cells). The obtained data indicated that porosity and hepatic-specific functions of the printed liver microtissues were significantly increased in GelMA/dECM bioinks compared to GelMA bioinks. It has been demonstrated that hepatocytes require a scaffold with at least 95% porosity to maintain high metabolic functions[10]; pore sizes of 10 or 80 μm improve the hepatic function in rat hepatocytes. Moreover, the metabolic function increased with 80 μm pore sizes, especially at a high cell concentration, due to the increased cell–cell interaction resulting from larger pore sizes.[11] The impact of different dECM hydrogel properties on cellular behaviors is summarized in Table 1.

2.2. Chemical composition and matrisome

Baptista et al. reported that the total composition of decellularized liver contained ≈0.5% of sulfated glycosaminoglycans (sGAG), ≈73% of collagen, and ≈23% of elastin (by dry weight).[14] However, in recent

Table 1. Impact of different dECM hydrogel properties on cellular behaviors.

Property	Material	Impact on cellular behavior	Ref.
Pore size	Collagen foam	The pore size of 10 or 80 μm improves the viability of rat hepatocytes	[11]
Porosity	GelMA/liver dECM	Higher porosity maintains the increased viability of HiHeps after 5 days of cultivation	[9]
Normalized storage modulus	Porcine lung dECM hydrogel	Gels with higher storage modulus can contain more cells (PVECs, hLFs, or hMSCs)	[32]
Elastic modulus	Porcine UBM Pocine and SIS	dECM hydrogels with high elastic modulus maintained viable and elongated cells for 5 days	[12]
Stiffness	Collagen hydrogel with genipin	Mouse mesenchymal stromal cells on 10 mM genipin-mixed collagen gels: mouse mesenchymal stromal cells differentiated to vascular smooth muscle cells; 0 mM genipin-mixed collagen gels (≈0.0292 kPa): mouse mesenchymal stromal cells differentiated to visceral smooth muscle cells.	[13]

Abbreviations: AM, a*cetyl methoxy methyl ester group;* dECM, decellularized extracellular matrix; GelMA, gelatin methacryloyl; HiHep, human induced hepatocytes; *PVECs, pulmonary vascular endothelial cells; UBM, urinary bladder matrix; SIS, small intestine submucosa.*

years, detailed studies of the ECM and the discovery of new interactions led to the emergence of the "matrisome" concept. Matrisome is defined as a set of all ECM elements and ECM-associated proteins.[15] It is important to consider the main structural units of the normal liver matrisome to justify the choice of composition when creating tissue-engineered structures.

The matrisome is divided into the main matrisome of the ECM, consisting of collagens, glycoproteins, proteoglycans (PGs), and other components, such as matrix-bound vesicles (MBVs[16]), and matrisome-associated molecules, which are divided into ECM-secreted proteins (e.g., transmembrane PGs, collagen-related proteins, cytokines, transforming growth factor β [TGFβ]) and ECM regulators (enzymes that destroy or change the structure of the ECM, e.g., matrix metalloproteinases [MMPs], α1-antitrypsin).[15,17] Therefore, the ECM is not only responsible for maintaining the structure and supporting cells, but also provides a reservoir for growth factors and cytokines and acts as a signaling core, where each cell can communicate with its environment and other cells.[18,19] The most important ECM components include PGs, glycosaminoglycans (GAGs), glycoproteins, collagens, bioactive collagen fragments, and integrins.

Proteoglycans (PGs) are divided into four main subclasses, which determine their various functions: extracellular, intracellular, pericellular, and cell surface-associated.[18–20] Their main functions are similar to the co-receptors of signaling molecules, regulating the integral properties of cells, such as adhesion, migration, proliferation, angiogenesis, and viability. The subclasses and functions of PGs are summarized in Table 2.

Glycosaminoglycans (GAGs) represent a part of PGs and an important component of the ECM, usually not found in free form. In the liver tissue matrisome, the main representatives of the class are heparin sulfate and HA[21]; HA is synthesized by stellate cells of the liver and immediately released into the extracellular space.[15] This is a process highly controlled by enzymes located on the inner surface membranes of stellate cells.[22] HA plays an important role in the formation of the normal structure of the ECM, controlling tissue hydration and maintaining the osmotic balance.[22]

The typical representatives of glycoproteins are adhesive proteins, e.g., fibronectin, laminin, and elastin. They ensure cell adhesion inside the ECM through the interaction with membrane receptors. In the liver tissue, glycoproteins are mainly represented by fibronectin 1 (FN1), elastin and elastin microfibril interface located protein 1 (EMILIN1), periostin, tenascin, fibrillin (FBN1), fibrinogen alpha, beta and gamma chains (FGA, FGB, FGG, respectively).[17] Laminin, a component of the basement membrane of the liver, is represented by seven different chains, but is often found in large quantities in pathological liver tissues, e.g., fibrosis.[17,23]

Different types of collagens are a part of both the basement membrane and interstitial tissue. The components of the basement membrane are chains of collagen IV and collagen VI.[17] The other collagens are detected in different concentrations, depending on the specific sample, the accuracy of the study, and other factors. In a mass spectrometry study, fibrillar collagens I, III, V, and XXVII were detected (and considered the most common); fibril-associated collagens with interrupted triple helices (FACIT) IX, XII, XIV, XVI, XIX, XXI, and XXII (the least common and variable in their presence in the liver tissue); collagens VIII and X form networks.[17] The origin and roles of the various proteins are only partially

understood. For example, collagen VIII is synthesized by endothelial cells and vascular smooth muscle cells.[15]

Moreover, collagen fragments are the key players in cell signaling and tissue remodeling. The most well-known molecules of this class are MMPs (matrixins), tissue inhibitors of metalloproteinases (TIMPs), and disintegrins and metalloproteinases with thrombospondin motifs (ADAMTS).[15,24] MMP and TIMP are in physiological equilibrium in the normal liver tissue. MMPs degrade various types of extracellular collagen, while TIMPs regulate MMP activity through hydrolysis.[22] Thus, a normal ratio of MMP and TIMP regulates the ECM composition and inhibits the process of liver fibrosis.[24] Eight types of MMPs are found in the liver tissue, namely, MMP-1, MMP-2, MMP-3, MMP-7, MMP-8, MMP-9, MMP-12, and MMP-13, each of which performs specific functions in maintaining the normal ECM composition.[12] The role of the ADAMTS2, ADAMTS3, and ADAMTS14 enzymes is to cleave aminopropeptides of fibrillar procollagens, promoting collagen maturation and formation of normal ECM.[15]

The function of integrins (transmembrane cellular proteins) is to bind the ECM and cell cytoskeleton, transmit signals into cells, and interact with other ECM molecules.[15] They consist of alpha and beta subunits, which are further divided into different types, determining their role in modeling the liver tissue.[15,25]

3. Preparation of dECM hydrogels for 3D bioprinting

3.1. Classic preparation methods for dECM hydrogels

Methods for producing dECM hydrogels can be divided into the following groups: (i) solubilization of the prepared dECM in the form of a fine powder with pepsin in hydrochloric acid (Freytes et al. method[26]), or pepsin in acetic acid (Voytik-Harbin method[27]); and (ii) the Uriel method,[28] which consists of isolating the ECM as a product of tumor tissues (Figure 1).

In Freytes et al.[26] method, pepsin is used to release collagen monomers into the solution, since pepsin cleaves the terminal telopeptides present in the triple helix of collagen with "unfolding" of collagen fibrils. The dECM, according to the Freytes et al.[26] method, is first crushed to a fine powder (recommended particle size: 0.2–0.4 mm[29,30]), after which it is cleaved with pepsin in 0.1 or 0.01 N HCl for 48 h at room temperature (RT)[31] or predominantly for 72 h.[8] An alternative is the Voytik-Harbin method, which uses 0.5 M acetic acid as a medium for pepsin.[27] The duration of enzymatic hydrolysis is a key parameter; insufficient hydrolysis leaves most collagen in the form of dissolved aggregates, while excessive hydrolysis leads to predominance of low molecular weight products (less than 250 kDa) over high molecular weight products (above 250 kDa).[32] Other important parameters include the factors affecting collagen polymerization, such as temperature, ionic strength, and pH. Johnson et al.[31] studied the effect of changing one of the neutralization parameters of the myocardial dECM hydrogel and revealed that the gelation time can range from 20 min at low salt concentrations (0.5× phosphate-buffered saline [PBS]) to more than 8 h at high salt concentrations (1.5× PBS). In addition, increasing the salt concentration led to a two- to three-fold decrease in the storage modulus (G'). The same authors demonstrated that gelation slows down at 22°C, in contrast to collagen hydrogels, which have a gelation temperature range of 4–37°C.

The Uriel method involves the extraction of proteins and glycoproteins by homogenization in a high-salt buffer, disintegrating ECM particles, and collagen fibers at neutral pH.[33] The tissue is cut into small sections

Table 2. PGs of the liver and related organs.

Group	ECM molecule	Matrix phenotype	Functions
Pericellular/BM PGs	Collagen XVIII (liver)	Basement membrane	Inflammation; cell adhesion
	Agrin (gallbladder)	Basement membrane	Postsynaptic differentiation; depolarization at CNS synapses
Cell surface PGs	Syndecan-1 (liver)	Interstitial connective tissue	Angiogenesis; wound healing; cell invasion; and survival
	Syndecan-2 (liver)	Interstitial connective tissue	Actin cytoskeleton; cell adhesion
	Syndecan-4 (liver)	Interstitial connective tissue	Wound healing; cell invasion and survival; focal adhesion and stress fibers
	GPC-6 (liver)	Interstitial connective tissue	Cell growth; cell division
Intracellular PGs	SRGN (endothelial cells)	Interstitial connective tissue	Secretion of inflammatory regulator; formation of mast cell secretory granules; storage of growth factors and cytokines in secretory vesicles; tumor growth

Abbreviations: BM, basal membrane; CNS, central nervous system; GPC-6, glypican-6; PGs, proteoglycans; SRGN, serglycin.

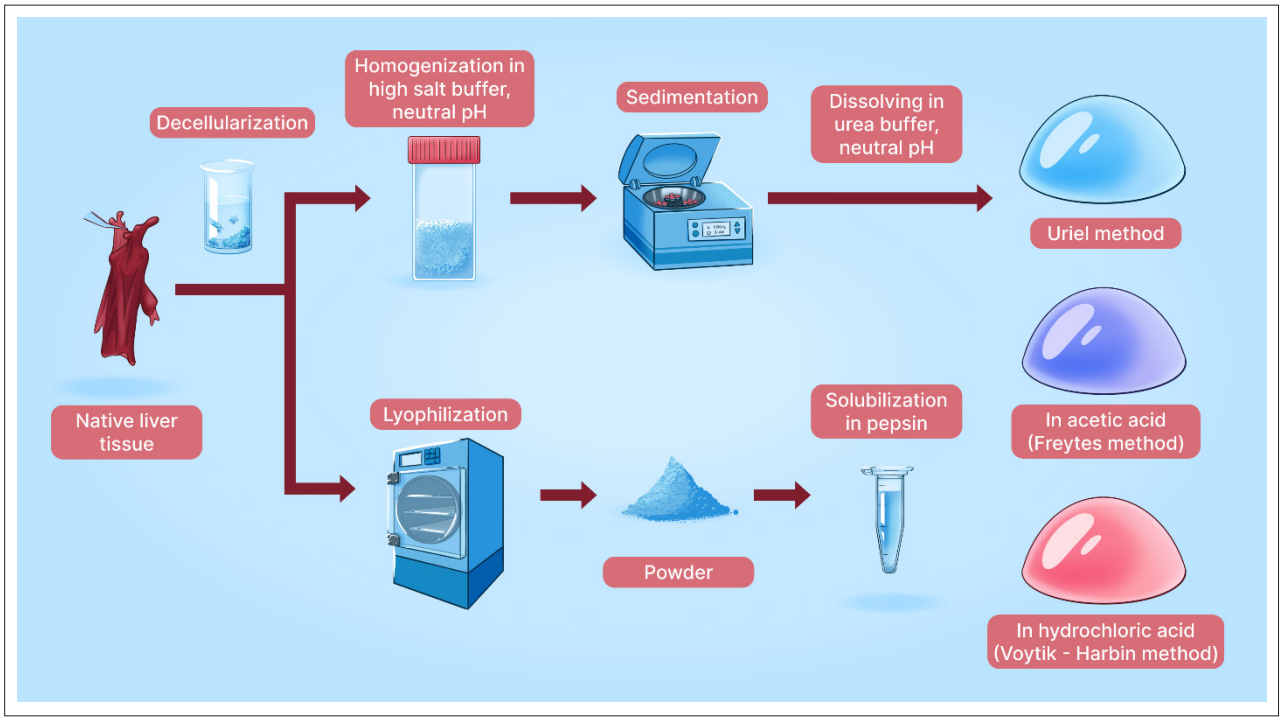

Figure 1. Approaches to obtain decellularized extracellular matrix (dECM) hydrogel via tissue homogenization in buffers (top) or solubilization in pepsin (bottom).

(1–2 mm thick), suspended in a dispase solution at a 2 mL/g tissue concentration, and incubated for 15 min at 4°C. The sections are passed through a cell sieve to separate cells from the remaining tissue. The tissue is homogenized in a high-salt buffer solution (0.05 µM Tris, pH 7.4, 3.4 M sodium chloride, 4 µM EDTA, and 2 µM N-ethylmaleimide), containing protease inhibitors (0.001 µg/mL pepstatin, 0.01 µg/mL aprotonin, 0.001 µg/mL leupeptin, 2 mM sodium orthovanadate, and 1 mM phenylmethylsulfonyl fluoride [PMSF]). The homogenate is centrifuged three times at 7000 × *g* for 15 min, and the supernatant is removed. The sediment is dissolved in a 2 M urea buffer (with the addition of 0.15 M sodium chloride and 0.05 M Tris, pH 7.4) at the amount of 1 mL of buffer per 1 g of tissue and stirred overnight at 4°C. They are then centrifuged again at 14,000 × *g* for 20 min; the supernatant is saved, and the sediment is resuspended in the urea buffer. The sediment is homogenized and centrifuged again at 14,000 × *g* for 20 min. The supernatants from both centrifugation steps are used in subsequent experiments.[33]

3.2. Alternative methods for producing dECM hydrogels

Considering the original method of Freytes et al.[26] without modifications reveals inconsistencies regarding the potential clinical translation of dECM-derived hydrogels. For instance, although porcine mucosa pepsin is irreversibly denatured at pH 7.0–7.4, it should be completely removed, as residual pepsin can cause allergy and inflammation. Additionally, pepsin cleaves collagen in non-helical regions where telopeptides are located, suggesting that collagen telopeptides with pepsin should also be removed. Besides that, the decellularization and lyophilization processes should be as mild and accurate as possible to ensure cell removal and preservation of GAGs, PGs, basement membrane components, and secreted factors.

3.2.1. Modified preparation methods for dECM hydrogels

Modifications to the methods for producing dECM hydrogels include the enzymatic breakdown of the ECM with acidic pepsin. For example, Simsa et al.[30] used the Freytes et al. method in their study. Briefly, lyophilized pig brain tissue was ground to a powder using a knife mill with a 60-mesh sieve to sift particles with a size of 250 µm, followed by enzymatic hydrolysis of the ECM in 0.1 M HCl and pepsin (enzyme:substrate ratio = 1:10). After 72 h of hydrolysis, the suspension was centrifuged at 13,000 rpm for 10 min; the supernatant was collected and neutralized to pH 7.2–7.8 in an ice bath with the addition of 1/10 volume of 10× PBS. The solution was then quickly frozen and lyophilized. The lyophilizate of the porcine brain dECM hydrogel was also ground using a knife mill and a 60-mesh (250 µm) sieve, after which the resulting

particles were dissolved in distilled water and vortexed, then incubated at 37°C to form a hydrogel (Figure 2). The final G' of hydrogels were 0.7, 12.8, and 36.4 Pa at concentrations of 5, 10, and 15 mg/mL, respectively. A linear dependence of the G' on the strain was observed up to 10% strain, and the change in the G' did not exceed 5% within this range. This value is similar to that of Matrigel, which has a linearity range of up to 13%.[30] However, regarding this particular modification, it should be noted that the second lyophilization step could lead to gelation failure in case of poor lyophilization post-digestion.

Another modification of the standard Freytes et al.[26] method was proposed for the preparation of porcine intestinal hydrogels for an endodermal organoid model.[34] Decellularized porcine intestinal matrix was lyophilized for 72 h, ground to a fine powder using a knife mill and a 40-mesh (0.4 mm) sieve, then sterilized by γ-irradiation and stored at −20°C until use. For solubilization, various concentrations (4, 6, 8, and 10 mg/mL) of porcine intestinal dECM powder were dissolved in a solution of pepsin in hydrochloric acid (1 mg/mL in 0.1 M HCl) at RT for a 72-h incubation. The acidic pre-gel was centrifuged at 200–400 × g for 5 min to remove incompletely cleaved particles. To mix with isolated intestinal crypts, the pre-gel solution was brought to an isotonic salt concentration by adding 10% 10× DMEM F/12 or 10× PBS, then titrated with 10 N NaOH with thorough mixing; neutralization was carried out using cut tips (Figure 3). The gel was mixed with cell sediments and aliquoted in 30–40 µL into a Petri dish, and the gelation time was not longer than 30 min. The authors emphasize that the pre-gel stored at RT was not able to form a gel, unlike the one stored at 4°C. The 6 mg/mL dECM gel had properties similar to those of Matrigel (storage and loss [G''] moduli; elastic modulus) and was used for culturing organoids.[34]

Ijima et al.[35] used the Freytes et al.[26] method to produce liver dECM hydrogel; 10 mg of the lyophilized liver matrix was hydrolyzed in 1 mL of pepsin at a concentration of 1 mg/mL in 0.1 N HCl, and the hydrolysis was carried out for 72 h at 4°C. The pH of the acidic pre-gel was

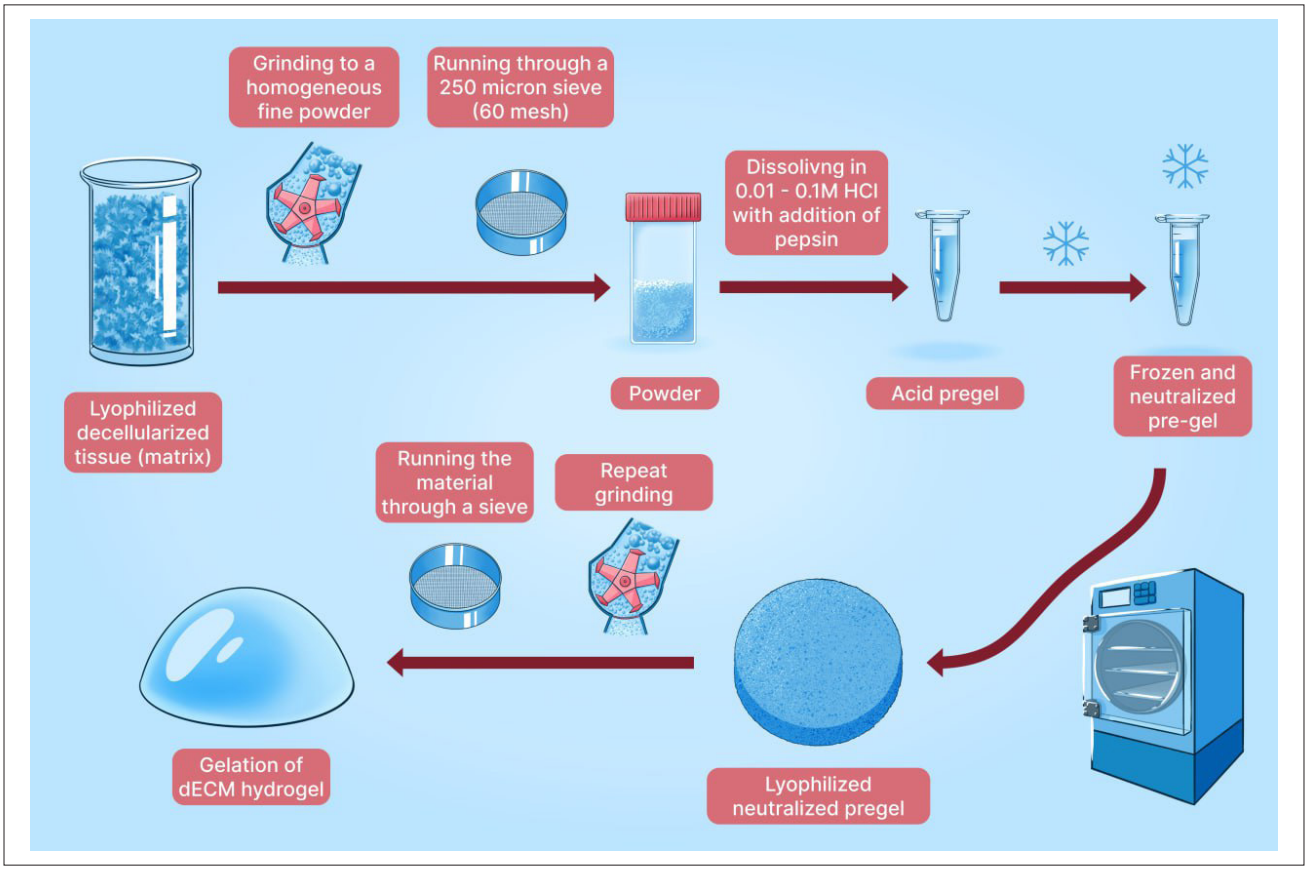

Figure 2. A modification of the Freytes method by Simsa et al.[30] This modification was used for the porcine brain decellularized extracellular matrix (dECM) hydrogel formation and the subsequent culture of cerebral organoids inside the hydrogel. Notably, the authors used a second lyophilization step after the acid pre-gel neutralization, balancing the salt concentration.

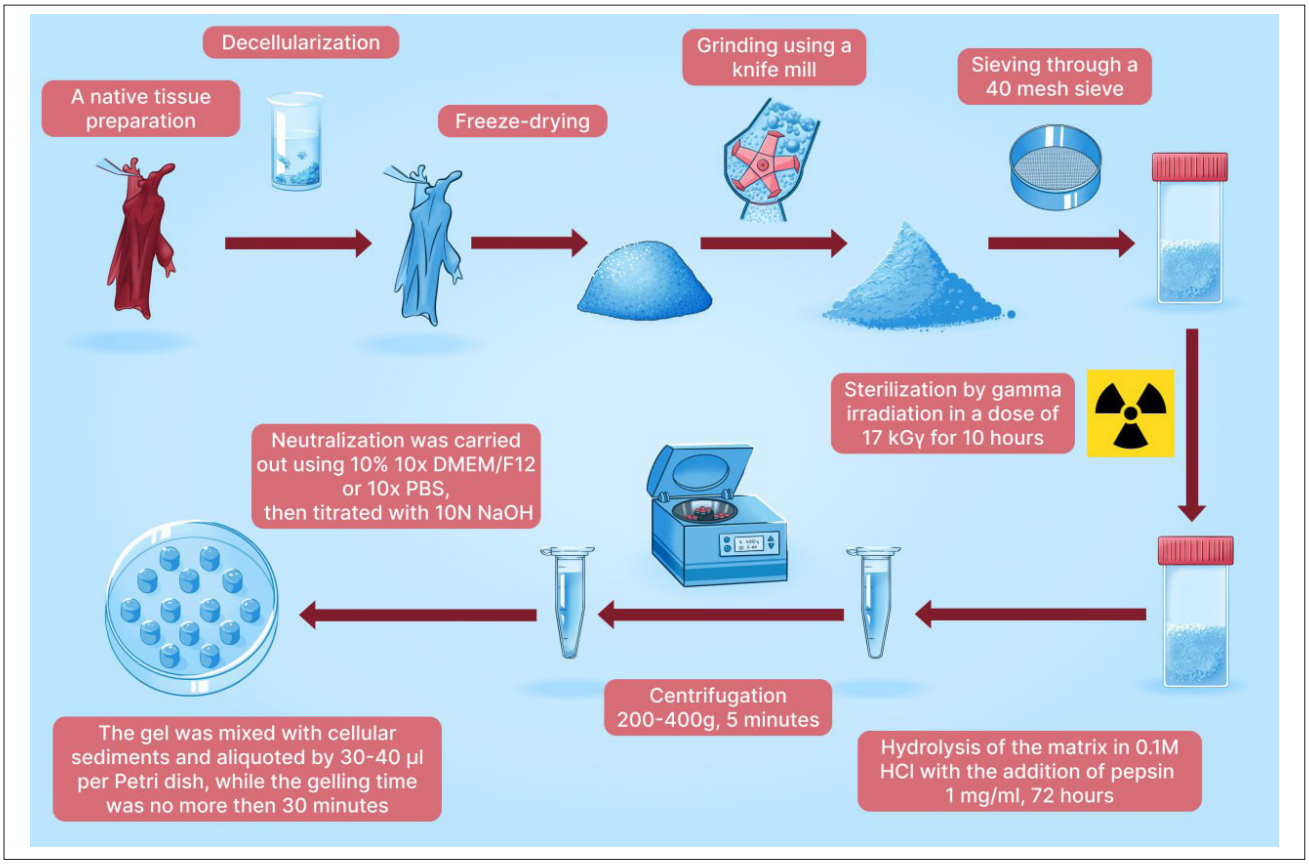

Figure 3. A modification of the Freytes method used by Giobbe et al.[34] Lyophilized, ground, and sieved porcine small intestinal matrix was sterilized by gamma irradiation for 10 h at 17 kGy. Gamma sterilization is a distinct step in this protocol as it is generally excluded in most studies.

adjusted to 3.0 by dialysis. The pre-gel was mixed with the neutralization buffer (47.7 mg/mL HEPES; 0.08 N NaOH) and concentrated nutrient medium (10× MEM, in a volume ratio of 8:1:1) and incubated in an ice bath. Gelation was observed during a 30-min incubation at 37°C. The authors conducted studies using three groups of samples: (i) acid-soluble telocollagen; (ii) pepsin-soluble collagen, and (iii) porcine liver dECM. Pepsin-soluble collagen had a constant G' value in the strain range of 0.1%–20%. However, when the strain was increased above 20%, G' decreased sharply with a simultaneous increase in G'', and this phenomenon was concentration-dependent. Porcine atelocollagen at a concentration of 1 mg/mL did not exhibit G' crossing G'', indicating a relatively viscous state. However, at a concentration of 2 mg/mL, an intersection of G' and G'' was observed, demonstrating that elastic behavior became more pronounced with increasing concentration. For the liver dECM hydrogel, the range of linear viscoelasticity appeared narrower, ranging at 0.1%–10%. In addition, an increase in G' and G'' at high frequencies was recorded for both telocollagen and liver dECM. In comparison with pepsin-soluble collagen, the G' and G'' did not intersect in the measured frequency range. When comparing acid-soluble collagen type I (3 mg/mL) and liver extracellular matrix (L-ECM; 10 mg/mL), comparable fiber densities were noted. The fiber diameter in the 3 mg/mL collagen gel sample was larger compared to that for the liver dECM, but the fiber density in the 20 mg/mL liver dECM hydrogel was higher compared to that for the 10 mg/mL hydrogel. The authors suggest that the diameter of the fibers depended on the presence of additional ECM components other than collagen, while the density depended on the concentration.

3.2.2. Alternative methods to obtain dECM

Higher-quality dECM hydrogels can be produced using alternative decellularization methods instead of chemical techniques. For instance, a custom laboratory-scale ultrafiltration system was used to concentrate a porcine dermis atelocollagen solution and remove both telopeptide and pepsin.[36] The dermis layer of the porcine skin was sliced and then placed in a $scCO_2$ vessel system containing 75% ethanol as a co-solvent. After the decellularization step, the obtained dermal membrane was freeze-dried and sterilized by γ-irradiation. After that, the minced dermal membrane

was treated with a continuous flow of liquid nitrogen and fed to a freeze-miller. Sieved particles of 50–200 μm sizes were collected and sterilized again by γ-irradiation. Freeze-milled powders were soaked in pepsin (1 mg/mL in 10 mM HCl, pH 2.0) and shaken for 16–18 h at 25°C. The obtained acidified atelocollagen solution was filtered using the lab-built ultrafiltration unit consisting of two columns; the first column blocked and removed particles larger than 1.4 μm, and the second one retained proteins with molecular mass higher than 150 kDa. With the use of the second column, the atelocollagen solution was concentrated by successive runs of 0.1 N HCl. To adjust pH to 7 and induce the fibrillogenesis, nine parts of the sterilized atelocollagen solution were mixed with one part of 0.2 M phosphate buffer, and the obtained precipitate was centrifuged to form an atelocollagen slurry, which was then freeze-dried to form an atelocollagen powder. This process of atelocollagen preparation can be considered as a process with minimal manipulation, unlike traditional laborious and time-consuming processes, where salting-out, alkali, acid, and enzymatic treatments, as well as ion-exchange chromatography, were used.

Interestingly, Hussey et al.[37] proposed a new method for the preparation of dECM hydrogels using ultrasonic cavitation instead of the traditional mild-acidified pepsin digestion. Lyophilized and milled dECM was used as a starting material; dECM was resuspended in a neutral buffered salt solution and dissolved by sonication.[37]

In dECM stock production, apart from removing pepsin and telopeptides, there is a need to streamline the process for clinical translation. For example, a second lyophilization step is proposed to standardize and ease the manufacturing process.[30] This modification of the Freytes et al.[26] method facilitates the formation of stock material for dECM hydrogel preparation and long-term storage of the stock dECM material.

3.3. Gelation process of dECM hydrogels

After the preparation steps, dECM-based hydrogels undergo polymerization under standard conditions of neutral pH and a temperature of 37ºC. It should be noted that the exact mechanism of gelation of ECM hydrogels, as well as the role of pH and temperature factors, have not been precisely established. Although the kinetics of the self-assembly of collagen fibers upon changes in the pH and temperature are known, the role of other ECM components in collagen assembly cannot be ignored. Voytik-Harbin and Brightman[27] demonstrated that ECM hydrogels are characterized by self-assembly kinetics, network structure, and fiber morphology different from those of purified type I collagen. For example, the addition of sGAG, heparin in particular, or PGs (decorin), to purified type I collagen revealed that heparin promotes faster collagen gelation and fiber thickening. Decorin also increases the rate of collagen gelation, but does not affect either the thickness of fibers or their compaction.[27] These results are consistent with the known function of heparin as a nucleation site for collagen fibrillogenesis, and of decorin as a regulator of collagen fiber self-assembly.[38] In addition to heparin and decorin, many other ECM proteins also affect collagen assembly; fibronectin and minor types of collagens (collagen V and XI) are known as nucleation sites, the presence of which is necessary for *in vivo* collagen fibrillogenesis.[39]

However, dECM hydrogels, similar to type I collagen, are subject to *in vitro* degradation to a greater extent compared to composite hydrogels. For example, Kayabölen[40] measured the degradation kinetics of decellularized adipose tissue hydrogels with the addition of silk fibroin (3:1, 1:1, and 1:3, respectively) and indicated that the 1:3 gel was much more resistant to degradation compared to the 1:1 gel.

Secondly, these biomaterials, depending on the duration of enzymatic hydrolysis and other parameters, may exhibit insufficient elasticity. Low G' was reported for porcine lung dECM hydrogel obtained after 72 h of hydrolysis in acidic pepsin. A rheological study revealed higher and more stable G' for aliquots of the hydrogel taken at 4, 12, and 24 h of hydrolysis, while a drop in G' was recorded for aliquots from 48 to 72 h of hydrolysis.[32]

Thirdly, furthermore, dECM-based hydrogels can harden unevenly and slowly during the bioprinting process, which, combined with a significant nozzle diameter (0.4 mm) and high printing speed, can lead to the collapse of the construct. Additionally, slower gelation of dECM hydrogels has been reported with excess NaOH.[41]

3.4. Modifications used to control the viscosity/ crosslinking of dECM hydrogel

The above circumstances emphasize the need for modifications of dECM hydrogels, which may have a physical or chemical mechanism.

3.4.1. Genipin crosslinking of collagen

The mechanism of crosslinking of collagen and dECM by genipin has not been fully understood. One of the proposed mechanisms includes two stages; in the first stage, a nucleophilic attack of an amino group in the collagen chain on the olefinic part of the α,β-unsaturated ester in the genipin molecule takes place, opening of the genipin ring; then, an amino group of another collagen chain attacks the methoxycarbonyl group to form an amide bond, thus crosslinking the two collagen chains.[42,43]

Genipin, due to its low toxicity compared to glutaraldehyde, is used in the preparation of crosslinked

dECM hydrogels. For example, Boso et al.[44] lyophilized a decellularized diaphragm powder (1%, 2%, and 3%), which was subjected to enzymatic hydrolysis with the addition of up to 10% pepsin in 0.5 M acetic acid for 48 h. To restore the osmolarity and physiological conditions, the pre-gel was titrated to pH 7.4, followed by the addition of 10% 1× PBS. After hydrogel formation, 1 mM genipin in 1× PBS was immediately added and incubated overnight; the hydrogels were washed three times with 1× PBS to remove the residual genipin. Crosslinking using genipin can be monitored by recording fluorescence at an excitation wavelength of 590 nm and an emission wavelength of 630 nm. The same authors indicated that hydrogels crosslinked with genipin demonstrated denser organization of fibers compared to non-crosslinked hydrogels; a twofold increase in viscosity was observed compared to the non-crosslinked hydrogel of the same concentration. In addition, the crosslinked hydrogels exhibited elastic properties to a greater extent than the non-crosslinked gel.[44]

3.4.2. Crosslinking with "zero-length" chain agents

Another frequently used method is crosslinking with bifunctional crosslinkers, 1-ethyl-3-(3-dimethylaminopropyl)carbodiimide (EDC), and N-hydroxysuccinimide (NHS) esters.

EDC, the former reacts with a carboxyl group to form an active O-acylurea intermediate, which is then displaced by the nucleophilic attack of a primary amine. The primary amine then forms an amide bond with this initial carboxyl group, releasing a soluble urea derivative. The O-acylisourea intermediate is unstable in aqueous solutions. NHS and its water-soluble analog (sulfo-NHS) are often used to react with EDC, creating more stable NHS esters. These NHS esters react with primary amines, forming an amide bond and subsequently releasing NHS.

Although EDC and NHS esters both are "zero chain length" crosslinkers, the mechanism of crosslinking cannot be considered biocompatible, since cell culture media contain primary amines. Nevertheless, EDC and NHS were used to crosslink a polyamidoamine dendrimer into which HeLa and 3T3 cells were encapsulated, and cell survival on the second day was 80%.[45]

3.4.3. Photopolymerization

Photopolymerization is a common method for crosslinking of bioprinted hydrogels, allowing for high-precision polymerization control of 3D structures. In order to induce free radical polymerization with chain growth, as well as step-growth polymerization, additional functional groups are introduced into the ECM, like acryloyl chloride, methacryloyl chloride, methacrylic anhydride, 2-isocyanato-ethyl methacrylate, glycidyl methacrylate, 5-norbornene-2-carboxylic acid, cysteine derivatives, dithiothreitol, 3-mercaptopropionic acid, etc.[46]

The first mechanism to be considered is free radical photopolymerization with chain growth. It is known that macromolecules containing a vinyl group are capable of photopolymerization as the chain grows.[46] Irradiation at the appropriate wavelength leads to the absorption of light energy by the photoinitiator and its dissociation with free radical formation. These free radicals attack the vinyl groups of the macromolecular precursor, leading to the homolytic opening of the π bond, thereby forming new free radicals. Therefore, the reaction center spreads as covalent bonds between precursors are completed, which contributes to the formation of a polymer chain from several seconds to minutes. Typically, photopolymerization occurs under ultraviolet (UV; 365 nm) or high-energy visible light (405 nm). Although free radical chain growth photopolymerization has been successfully used to obtain 3D cell constructs, the photopolymerization conditions must be carefully selected. It was reported that cell survival in the presence of several photoinitiators depends on the cell type and growth rate. Irgacure 2959 (2-hydroxy-1-(4-(2-hydroxyethoxy)phenyl)-2-methylpropan-1-one) turned out to be one of the least cytotoxic photoinitiators and the most commonly used for cell encapsulation. However, Fedorovich et al.[47] observed unfavorable effects of this photoinitiator on mesenchymal stromal cells (MSC) monolayer. Similarly, Rouillard et al.[48] demonstrated that free radicals generated by this photoinitiator negatively affected cell survival, which was reduced by up to 70%. Another commonly used photoinitiator, lithium phenyl(2,4,6-trimethylbenzoyl)phosphinate (LAP), is less toxic due to its maximum absorption in the near-UV region (i.e., 365 nm).

The second mechanism, step-growth photopolymerization, is used conventionally to produce collagen-based hydrogels. It is known also as thiol-ene polymerization and requires the presence of two functional groups, vinyl and thiol.[46] Thiol-ene is conducted under the same conditions as free radical polymerization, often photochemically induced. It resembles a typical chain process with three stages: initiation, propagation, and termination. Initiation involves the decomposition of the photoinitiator into free radicals, which attack the thiol group and forms thiyl radicals (RS) and other byproducts. Propagation consists of two stages; a thiyl radical attacks C=C double bond, forming the intermediate carbon-centered alkane radical that attacks another thiol group to obtain the thiol-ene addition product, regenerating the thiyl radical. The termination reactions involve radical–radical coupling processes. The step-growth photopolymerization process is considered to be more

cell-compatible compared to radical chain growth polymerization,[46,49] as it is associated with low reactive oxygen species (ROS) levels. When choosing (meth) acrylate as a vinyl group for thiol-ene polymerization, step-growth polymerization is not the only approach, as free radicals of the photoinitiator can interact with both thiol and methacrylate groups. Anseth et al.[50] studied the formation of thiol-methacrylate networks during mixed polymerization, as well as the mechanical properties and degradation kinetics of the resulting gels; these gels were used to encapsulate MSCs. As a result, the gel was obtained by mixed polymerization with the addition of cell adhesion peptides containing cysteine. Additionally, the preparation of a hydrogel consisting of thiolated heparin and methacrylated HA, which polymerizes under visible light, has also been reported.[50,51]

Regarding dECM hydrogels, slightly different approaches are used, the essence of which is to introduce functional groups into the dECM (most often [meth] acrylate) or by mixing with materials that improve the micromechanical properties of dECM. For example, Brew[52] functionalized placenta dECM after decellularization and enzymatic hydrolysis using methacrylation.

3.4.4. Physical modifications with interpenetrating polymer networks

The interpenetrating polymer network (IPN) is a polymer network consisting of two different polymer networks that are bound to each other at least partially but non-covalently. The hydrophobic, ionic, or hydrogen bonding inside the IPN is responsible for the improved mechanics and degradation behavior. There are some examples of generating IPNs with collagen and dECM. For instance, Shi et al.[53] utilized GelMA hydrogel to encapsulate chondrocytes and construct a phase transition 3D cell culture system, in which gelatin microspheres created micropores within the hydrogel. They demonstrated that after 28 days of culture, the GelMA phase transition culture system forms an ECM predominantly composed of collagen type II, collagen type I, and fibronectin. After decellularization, the protein types and mechanical properties are well preserved, fabricating a dECM-GelMA IPN that consists of GelMA hydrogel as the first-level network and the ECM secreted by chondrocytes as the second-level network. Crosby et al.[54] have synthesized an IPN hydrogel comprised of collagen and norbornene-modified HA (NorHA) (1 wt% NorHA and 0.25 wt% collagen). The approaches to modifications of dECM hydrogel are summarized in Figure 4.

4. Bioprinting of dECM-based constructs

As mentioned above, dECM hydrogels can reproduce the native microenvironment of stem cells and possess a biochemically unique signature of tissue-specific ECM. Hence, these hydrogels can be considered a base for bioink and a medium for expanding cells, spheroids, or organoids. Moreover, they can be regarded as GMP-compliant systems for 3D cell culture, in contrast to routinely used basement membrane extracts (BME)-related products obtained from tumorigenic cell lines.

The replication of bioprinted microtissues or structures depends on how close their architecture is to the anatomical features of their native counterparts. The complexity of the anatomical organization of tissues and organs, including multiple repeating functional units and at least several types of cells, defines bioprinting resolution as a crucial parameter for 3D tissue engineering. For liver lobule representation, the printing resolution should be high enough to generate a hexagon structure with 12 radial channels (liver sinusoids) and a central cavity; the total size of the lobule should not exceed 1.5 mm. For instance, this was achieved by Mao et al.,[9] who used a customized digital light processing (DLP) setup with a resolution of 200–500 μm.

The resolution of bioprinting is largely related to the technical characteristics of the bioprinter platform and the physicochemical properties of the bioink. Three main 3D bioprinting technologies include inkjet, microextrusion, and laser-based methods, namely laser-induced direct transfer (LIFT) technology, DLP, and stereolithography (SLA) technology. The resolution of inkjet bioprinting is determined by the contact angle of the surface; the speed of the nozzle in conjunction with the nonlinearity of viscoelastic properties has a decisive influence on microextrusion; and the resolution of printers with laser-based technology depends on the photo-crosslinking parameters and light characteristics.

The application of 3D printing technologies for organ-on-a-chip platforms has encountered difficulties in creating constructs that are physiologically comparable to native tissues at the desired resolutions, which are dictated by the detailed anatomical and physiological features of biological tissues. An ideal ECM-like microenvironment should have the following properties: (i) the pore size several times larger than the size of cells, which is necessary to create an adequate contractile force for cell motility; (ii) the pores must communicate with each other to ensure the diffusion of nutrients and metabolites; (iii) the appropriate surface chemistry must be maintained. In addition, it is crucial to maintain the accuracy of cell distribution, especially when using organs-on-a-chip for drug resistance research. The broad spectrum of approaches employed to create tissue-engineered liver via 3D bioprinting is summarized in Table 3.

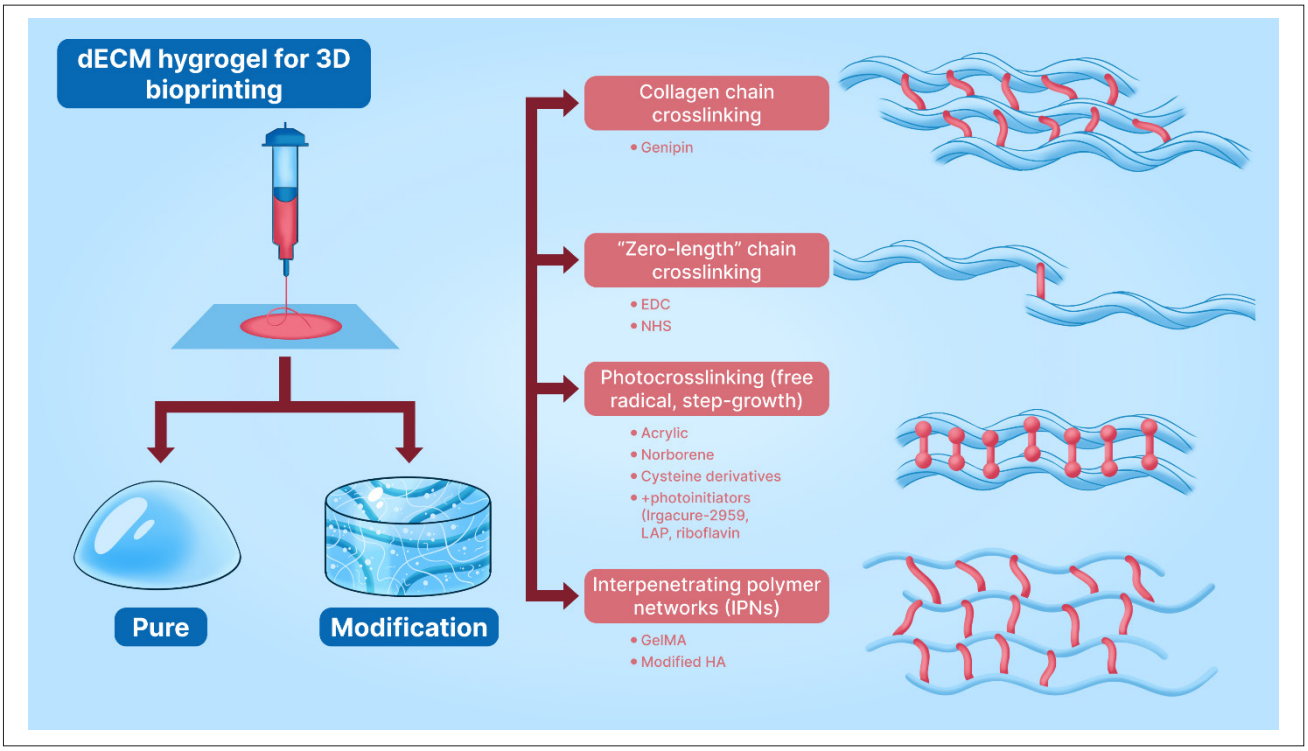

Figure 4. Major techniques of decellularized extracellular matrix (dECM) hydrogel modifications to improve mechanical properties. Abbreviations: EDC, 1-ethyl-3-(3-dimethylaminopropyl)carbodiimide; GelMA, gelatin methacrylate; HA, hyaluronic acid; LAP, lithium phenyl(2,4,6-trimethylbenzoyl) phosphinate; NHS, N-hydroxysuccinimide.

The cell patterning and organization in bioprinting are further complicated by multi-component designs required to reproduce highly vascularized organs and tissues (e.g., the liver). Cell patterning plays a critical role in liver tissue biofabrication because a functional liver is composed of multiple cell types, which necessitates the use of bioinks made from various materials and cell types in liver bioprinting. Liver sinusoids are distinct microvascular systems (less than 10 μm in diameter) lined by sinusoidal endothelial cells that form a radial pattern; they are critical for the survival and function of liver hepatocytes.[65] Accordingly, a similar resolution of about 10 μm is required to reproduce hepatic and liver sinusoidal cell patterns.

In addition to the difficulties associated with reproducing cellular patterns and microenvironments, bioprinting is also challenged from other aspects, such as increased printing speed, printing using multiple types of materials and cells, and the need to minimize shear strain on cells. Taken together, these factors may contribute to the loss or reduction of resolution in the final construct. When bioprinting is used to generate support structures and microfluidic channels, the resolution provided by the technology platform, as well as the viscoelastic properties of the biomaterial, play a key role in the functioning of the organ-on-a-chip platform. The influence of various 3D bioprinting parameters on the resolution of constructs is discussed in detail below.

4.1. Inkjet bioprinting systems

In the case of droplet-jet bioprinting, the bioink is pressed through a nozzle with a small diameter, leading to bioink deposition in the form of individual droplets (Rayleigh–Plateau instability). These droplets become charged, and accordingly, an electric field is used to precisely position the droplets. For bioprinting of materials, drop-on-demand (DOD) bioprinters are used, which can be divided depending on the method of droplet formation: printers with a temperature or piezoelectric print head,[66] as well as inkjet printers that use ultrasound to form droplets of the material.[67]

The resolution of inkjet, mainly DOD, printers is determined by the size of a drop on a flat surface, from which the vertical and lateral resolution can be determined.[68] Several studies have demonstrated the ability of DOD bioprinting to generate high-resolution cell constructs with limitations on hydrogel viscosity (≤10 mPa/s) and cell number (≤10 million/mL).[69] Additionally, DOD inkjet bioprinting has been used to fabricate a liver-on-a-chip by patterning liver organoids.[70] Bioequivalents were represented by layers of human umbilical vein

Table 3. Summary of methodical approaches used for 3D bioprinting of liver constructs.

Bioprinting method	Material	Cells	Physiological activity	Printing parameters	Resolution (μm)	Ref.
DMD	(i) 5% GelMA for supporting hiPSC-HPCs; (ii) 2.5% GelMA with 1% GMHA for supporting cells	HPCs and HUVECs-ADSCs (50:1; 4×10^7 HUVECs and 8×10^5 ADSCs)	76% viable cells within 2 h following printing; 65% viable cells after a week; higher expression levels of HNF4α, TTR, and ALB in triculture	Size: 500 μm; height: 200 μm; first layer: HPCs in a 1:1 prepolymer of 10% GelMA; second layer: supportive cells in a prepolymer of 5% GelMA and 2% Glycidyl methacrylate-hyaluronic acid (GMHA)	50–200	[55]
Extrusion	3% alginate with 1% $CaCl_2$	Primary rat hepatocytes (4×10^7 cells/mL)	Viable culture after 14 days	Size: 25 × 25 mm (square); seven layers	200–500	[56]
	dECM with 10% GelMA and 0.5% LAP	hiHep cells ($2.5–3.0 \times 10^6$ cells/mL)	More live cells in dECM-incorporated bioink after 1 and 3 days of culture	Size: ~10 mm (round); height: 2 mm; protrusions (gear-like form)	200–500	[9]
	2% alginate with 3% gelatin and liver dECM (0, 0.25, 0.5, 1, and 2 mg/mL)	HepaRG (7×10^6 cells/mL)	Impairment of cellular metabolism at 2 mg/mL dECM	Size: 10 × 10 mm; H (height): 1 mm; regular pores	200–500	[57]
	Porous gelatin scaffold	Huh 7 (3.3×10^6/mL)	Higher ALB secretion for a layer orientation of 60° (compared to 90° and 2D control on day 7)	Size: 15 × 15 mm; nozzle diameter: 200 μm; *D* (distance) between filaments: 700 μm; *L* (layer thickness): 156 μm		[58]
	4% alginate; 20% gelatin	HepaRG (1×10^6 cells/mL)	Higher gene expression of differentiated HepaRG	Nozzle: 23G; printing speed: 150 mm^3/min.		[59]
	liver Liver dECM hydrogel; Pluronic F127 as a FRESH substrate	Immortalized cholangiocytes and Huh 7 spheroids	Cholangiocytes remained viable after 7 days of cultivation; the morphology (proliferation and branching) depended on Huh7 spheroid concentration in the area	Nozzle: 200 or 150 μm		[60]
	15% alginate; 6% Pluronic F-127	75% hepatoblasts, 20% induced endothelial cells, and 5% induced MSCs (1×10^7 cells/mL)	High levels of urea secretion in liver spheroids compared to a suspension of single cells	Size: 10 mm (donut-shaped); *H* (height): 5 mm; n (Needle): 20G	-	[61]
	GelXA LAMININK: gelatin, alginate, xanthan gum, and LAMININ 521	HepG2 (3×10^7 cells/mL)	Highest cell viability and proliferation capacity when printed with GelXA LAMININK521	Size: 3 mm (hexagonal); height: 2 mm; Nnozzle: 25G	-	[62]

(*Continue...*)

doi: 10.36922/ijb.4343

Table 3. Continue...

Bioprinting method	Material	Cells	Physiological activity	Printing parameters	Resolution (μm)	Ref.
	10% GelMA; PEG-bis-acryloyloxyacetate	HepaRG and human liver stellate cells (10×10^7 cells/mL)	High viability for 14 days of culture; Ki-67+ cells were detected, but their number decreased during cultivation	Size: 4 mm (hexagonal); height: 5 mm; 12 hollow channels inside every hexagonal structure	67.2	[63]
SLA	20% PEGDA (3400 MW) with 20 μM/mL acryloyl-PEG-RGDS	Hepatocytes ($5–15 \times 10^6$)	Inclusion of the synthetic RGDS peptide led to a 5-fold increase in ALB secretion	Size: 34 mm	-	[64]

Abbreviations: ADSCs, adipose derived stem cells; ALB, albumin; dECM, decellularized extracellular matrix; DMD: Digital micromirror device; FRESH, freeform reversible embedding of suspended hydrogels; GelMA, gelatin methacrylate; GMHA, glycidyl methacrylate-hyaluronic acid; GST, glutathione S-transferase; hiHep, human-induced hepatocytes; hiPSC-HPCs, human induced pluripotent stem cells-hepatic progenitor cells; HPCs, hepatocyte progenitor cells; HUVECs, human umbilical vein endothelial cells; LDH, lactate dehydrogenase; MRP-2, multidrug resistance-associated protein 2; MSCs, mesenchymal stromal cells; MW, molecular weight; PEGDA, polyethylene glycol diacrylate; PEG, polyethylene glycol; RGDS, Arg-Gly-Asp-Ser peptide; SLA, stereolithography; TTR, Transthyretin.

endothelial cells (HUVECs) and HepG2 cells, while layers of fibronectin and gelatin were used as scaffolds. The authors reported that, by using DOD in printed organoids, a resolution of about 400 μm was achieved. This resolution can be improved by using hydrophobic surfaces (i.e., those with a large contact angle).[70]

An important advantage of inkjet DOD bioprinting is that bioprinting is performed in a virtually non-contact manner, which reduces the risk of contamination.[71] Another advantage of inkjet bioprinting is the ability to reproduce cellular patterns with multiple cell types and hydrogels using different types of printing heads. Despite these examples, the main disadvantage of DOD bioprinting remains its low resolution in the context of 3D models and organs-on-a-chip.

4.2. Extrusion bioprinting systems

Microextrusion bioprinting is a biofabrication technology that uses compressed air pressure or a syringe pump to extrude a highly viscous liquid (or gel) containing biomaterials and/or cells. An ideal biomaterial for microextrusion bioprinting should exhibit pseudoplasticity and thixotropy.

Among the physical properties of bioinks, the dynamic viscosity plays an important role in achieving a good resolution, along with the "printing threshold" (initiating the release of the bioink from the nozzle and stable formation on the surface of the platform). Extrusion bioprinting supports hydrogels with a viscosity range from 1×10^2 to 1×10^9 mPa/s.[72] Another important factor determining the resolution of microextrusion bioprinting is the speed of a material passing through the nozzle (extrusion speed), which is influenced by the pneumatic pressure or plunger stroke speed. The extrusion speed also affects cell survival; for example, an extrusion speed of 0.5 mm^3/s (0.5 μL/s) was reportedly optimal for cell survival, considering factors such as the extrusion time and shear strain.[73]

In general, it is known that the maximum resolution of microextrusion bioprinting is 50 μm.[74] However, this resolution can only be achieved under near-ideal model conditions using non-biocompatible materials without a cellular component. Typically, when the cell suspension density is 10^7 cells/mL or higher, a nozzle with a minimum diameter of 200 μm should be used; accordingly, the final resolution of the construct is expected to be in the range of 200–500 μm.[74] Microextrusion bioprinting is often used to generate functional liver constructs (Table 4).

4.3. Laser-based bioprinting systems

Laser-based bioprinting systems include stereolithography, two-photon polymerization, digital light projection, and

Table 4. Analysis of extrusion printing of liver constructs.

Bioink type	Hydrogel composition	Cells	Results	Ref.
Liver-specific hydrogel/liver-specific cells	Gelatin/porcine liver matrix microparticles (size: 13.4 μm)	Fibroblasts 3T3, HUVECs, mouse hepatocytes	The addition of microparticles improved the mechanical properties and printability; cell survival and ALB secretion were higher compared to gelatin without microparticles	[75]
	Pig liver ECM hydrogel combined with type I collagen (pig dermis)	HepG2, bone marrow MSCs	Liver dECM hydrogel contributed to the survival of cells and more pronounced (compared to type I collagen) differentiation of MSCs into liver cells (assessed using markers HNF1α, HNF3β, HNF4α, ALB, AFP, TTR, and CK18)	[76]
	HA/gelatin/liver ECM crosslinked with PEG-based crosslinkers	Primary human hepatocytes, primary stellate cells, Kupffer cells	Constructs maintained a high survival rate and detectable levels of ALB and urea on day 14 of culture	[77]
Non-specific hydrogel/liver-specific cells	AlgianteAlginate/gelatin/human lung dECM	HepaRG	Cells maintained good viability, and metabolic and functional activities (ALB, CYP3A4); HepaRG cells were successfully transduced with AAV serotype 6 vectors	[57]
	Col I-MA/HA-SH	Liver stellate cells LX2, activated fetal HSCs, human hepatocytes	Functional activity (secretion of ALB and urea) was observed for 15 days	[78]
	Alginate	HepG2	Cells encapsulated in alginate proliferated (Ki67+) and expressed metabolic markers (ALB, ASGPR1, AFP, CYP1A2, TAT) during 21 days of culture	[79]
	Alginate	Mouse hepatocytes	Functional activity of cells (expression of ALB, CK18, ASGPR1, HNF4α, Foxa3) during 14 days of culture	[56]
	PCL (substrate)/atelocollagen (cell encapsulation)	Rat hepatocytes, HUVECs, human lung fibroblasts	Maintained cell functionality for 10 days; co-culture with HUVECs improved the functional properties of the constructs	[80]

Abbreviations: ALB, albumin; AAV 6, adeno-associated virus type 6 vectors; ASGPR1, Asialoglycoprotein receptor 1; CK18, Cytokeratin 18; Col I-MA/HA-SH, Collagen I-methacrylated/thiolated hyaluronic acid; dECM, decellularized extracellular matrix; ECM, extracellular matrix; HA, hyaluronic acid; HSCs, hepatic stellate cells; HUVECs, human umbilical vein endothelial cells; MSCs, mesenchymal stromal cells; PCL, polycaprolactone; PEG, polyethylene glycol; TAT, tyrosine aminotransferase; TTR, transthyretin.

volumetric methods.[81,82] Unlike microextrusion and inkjet methods, bioprinting using visible or UV light involves the delivery of the photon energy to the desired point, which leads to local polymerization of the construct at that point. Moreover, the resolution of these bioprinting methods ranges from a micrometer or less than a micrometer.[81,82] The features of each of these methods, as well as their disadvantages, advantages, and resolution, are summarized in Table 5.

4.3.1. Laser-induced forward transfer

In general, a LIFT bioprinter comprises three elements: a laser that generates pulsed beams, a radiation-absorbing layer, and the material on the back of the latter. Laser radiation is absorbed by a thin layer of absorbent material on a transparent substrate. Absorption of pulsed laser energy at the interface between the transparent donor and the absorbent layer results in the formation of vapor bubbles or mechanical waves that destroy the donor layer around the irradiated area, transferring the bioink dropwise to the collector.[84,85]

In a study conducted by Leva et al.,[82] LIFT technology was used to print Huh7 tumor cells on porous scaffolds made of collagen and GAGs. Scaffolds were prepared by lyophilizing a collagen suspension (5 mg/mL fibrillated collagen; 0.44 mg/mL chondroitin 6-sulfate dissolved in 0.5 M acetic acid). To deposit cells onto the surface of the scaffold, the following parameters were used: the diameter of the round laser spot was 60 μm, the distance between the donor layer and the substrate was 500 μm, and the laser pulse density required for printing cells on the scaffold was 530 mJ/cm^2. The authors demonstrated that the LIFT method allowed precise positioning of cellular patterns, as each drop deposited on the matrix had a diameter of 100 μm and included 16–20 cells; the cell viability was 100% within 2 h after the completion of printing.

However, the difficulty of controlled deposition of individual droplets is a major challenge of LIFT technology,

Table 5. Summary of laser-based bioprinting methods in liver tissue engineering.

Bioprinting method	Resolution (μm)	Viability (%)	Hydrogel composition	Examples of liver constructs	Ref.
LIFT	>>100	90–100	Porous collagen and GAGs as the substrate	Porous scaffolds made of collagen and GAGs	[82]
SLA	>50	85–90	GelMA GelMA/GMHA	3D hexagonal lobule-like liver structures with iPSC-derived hepatocytes, HUVECs, and AT-MSCs	[55]
DMD/DLP	<100	75–90	5% liver dECM with 5% GelMA	Liver constructs (3 × 3 × 250 μm) with hexagonal lobules containing round elements (portal triad and central vein); each hexagonal lobe (diameter: 1 mm) had sinusoidal sections with a width of 35 μm	[83]

Abbreviations: AT-MSCs, adipose tissue-derived mesenchymal stem cells; dECM, decellularized extracellular matrix; DLP, digital light processing; DMD, digital micromirror device; GAGs, glycosaminoglycans; GelMA, gelatin methacrylate; GMHA, glycidyl methacrylate-hyaluronic acid; HUVECs, human umbilical vein endothelial cells; iPSCs, induced pluripotent stem cells; LIFT, laser-induced forward transfer; SLA, stereolithography.

which limits its resolution to 100 μm. In addition, one of the problems with LIFT is the unwanted deposition of a "residue" from the absorbent layer.[85,86]

4.3.2. Stereolithography

Most SLA printers are configured in such a way that a light source cures a vat filled with liquid photoresin on a moving platform. As soon as one of the layers is polymerized, the stand is lowered to a specified distance (depending on the vertical resolution of the SLA printer) to polymerize the next layer. SLA bioprinting was originally used to generate bone tissue models. For example, an SLA bioprinter with a resolution of 100 μm was used to cure a biodegradable photopolymer, represented by diethyl fumarate, poly(polypropylene fumarate), and bisacylphosphine oxide (with an absorption maximum of 325 nm) as a model for the regeneration of a critical bone defect with a thickness of about 4 mm and a diameter of 50 mm.[87] Another study reported the use of SLA technology to fabricate 1 mm neural conduits with a resolution greater than 50 μm.[88] SLA is used in the rapid fabrication of microfluidic systems using transparent photopolymers. The main advantages of the SLA method include eliminating the need for substrates and enabling rapid prototyping. However, in general, the SLA method is rarely used in bioprinting and tissue engineering due to low resolution and poor biocompatibility.

4.3.3. Laser printing using a digital micromirror device or digital light processing

New technologies, such as continuous DLP or digital micromirror device (DMD), make it possible to generate dynamic masks through personal computer (PC)-controlled control of micromirrors, where polymerization occurs per unit volume of the photopolymer, accelerating the photo-crosslinking process. A DMD consists of millions of mirrors arranged in columns and rows. Upon exposure, the DMD mirrors can reflect or project the light, resulting in a light pattern. Each layer is cured based on the light pattern generated by the DMD chip, and the light is then modulated and passed through reduction lenses onto the photopolymer. After patterning each layer, the substrate is lowered by a movable stand into a container with the photopolymer; thus, the light pattern falls on the next layer. The resolution of this method is comparable to the size of single cells, which can reach up to 5 μm just by adjusting the laser power. This method allows the use of high-density cell suspensions (from several million/mL) compared to methods that use nozzles.[88]

Using DLP technology, Mao et al.[9] utilized 10% GelMA in combination with 3% or 1.5% porcine liver dECM as a composite bioink containing hiHep cells. All bioink types were characterized by remarkable cell viability, but the addition of liver decellularized extracellular matrix (ldECM) increased the number of living cells compared to pure GelMA.[9]

Ma et al.[89] used liver dECM as a bioink in conjunction with the DLP approach to engineer a hepatocellular carcinoma model. For bioink formulation, 5% GelMA and 5% liver dECM were mixed with HepG2/C3A cells. Hexagonal constructs with a height of 200 μm were fabricated using a custom DMD-based system.[89] Using DMD, Zhu et al.[90] produced pre-vascularized constructs with complex geometries and varying widths (<50 μm) and 50–100 μm, more than 50 μm, using endothelial cells that were encapsulated in a mixture of HA glycidyl methacrylate and GelMA.

4.3.4. Laser bioprinting using two-photon lithography

Two-photon lithography (TPL) is an emerging laser-assisted bioprinting (LAB) technology that provides the

highest resolution in the biofabrication of 3D scaffolds. Unlike traditional LAB technologies, TPL does not require composite optical systems or photomasks. On the contrary, this method uses a near-infrared ultrafast femtosecond laser. Multiphoton absorption occurs in a medium that transmits the emitted light and does not absorb the light of the specified laser length. With two-photon polymerization, the fabrication of 3D objects is not limited to the layer-by-layer method. Microstructures are created from a transparent photosensitive material that has high absorption in the UV range and is transparent in the infrared region. Thus, 3D free-form constructs can be reproduced using a high-intensity femtosecond laser when the simultaneous energy of two photons exceeds the absorption energy threshold of the photosensitive material.[90,91]

In particular, using polyethylene glycol (PEG) tetrabicyclonine as a sensitive photopolymer, channel structures were generated by the photodegradation of the photopolymer in accordance with the given pattern, with a lateral resolution in the 1 μm order.[91,92] TPL is a promising technology in the field of 3D bioprinting because it can reproduce microtissue patterns at submicron resolution.

5. Large-scale manufacturing of dECM hydrogels and clinical translation

Although many dECM-derived materials still require evaluation at the pre-clinical stage, numerous decellularized products have become commercially available (Apligraf, GraftJacket, AlloDerm, etc.). These decellularized materials are most commonly manufactured in the form of sheets. Implantation of decellularized sheets requires more invasive procedures compared to injectable forms of decellularized materials. In particular, ECM hydrogels have been increasingly studied for their potential for minimally invasive delivery. Their gel form is advantageous for filling abnormally shaped defects. In addition, dECM pre-gel can be injected into the surgical site, and at a human body temperature (37°C), the dECM pre-gel can rapidly form a dECM hydrogel, highlighting the use of these hydrogels as an injectable substance to treat local trauma or disease. However, there is only one clinical trial conducted to evaluate the safety/efficacy of dECM hydrogels, i.e., a decellularized myocardial matrix from Ventrix, Inc. (ClinicalTrials.gov identifier: NCT02305602). The study findings support the initial safety and feasibility of injecting VentriGel, an ECM hydrogel derived from porcine myocardium, in post-myocardial infarction patients with left ventricular dysfunction.[93] They conducted a first-in-man, single-arm, multicenter trial to demonstrate the safety, feasibility, and preliminary efficacy of percutaneous trans-endocardial delivery of VentriGel. The safety (absence of adverse events) and efficacy (i.e., treatment with VentriGel significantly increased the maximum walk distance with time post-injection at 3 and 6 months) of the injection therapy of MI with Ventrigel were validated.[93] Hence, dECM hydrogels can be potentially applied as hemostatic materials[94] because of their good temperature sensitivity and ability to form irregular porous reticular scaffolds at 37°C that mechanically seal the vascular breach and form a physical barrier. However, they have poor mechanical properties, which hinder their application in the field. Despite their disadvantages, dECM hydrogels are extensively studied and used in regenerating various types of tissues *in vivo*. The progress of translating dECM hydrogels towards clinical applications is summarized in Table 6.

Although dECM hydrogels are extensively studied and are attractive for clinical translation (Table 6), only one product has reached clinical trials. This circumstance could be related to the existence of many specific challenges in the clinical translation of these materials. Firstly, manufacturing standards are not well established for dECM hydrogels. Challenges may also arise from laboratory processes related to dECM hydrogel preparation, such as the absence of a standardized protocol for tissue decellularization (although there are standardized criteria for effective tissue decellularization, cell nuclei are not visible on histological slides and residual double-stranded DNA [dsDNA] content is less than 50 ng/mg dry mass[115]), the need for complete pepsin and telopeptides removal, sterilization of the dECM material, and adequate source of dECM. Additionally, challenges associated with upscaling from laboratory to manufacturing include inter-animal differences, the need for reducing biological burden, and the influence of different harvesting conditions on product quality.

5.1. Challenges in scaling up from laboratory to manufacturing

When designing biomaterials for regenerative medicine applications, including dECMs, it is important to consider the implications for manufacturing, namely, increased costs, availability of raw materials, or difficulty of production. Animal-to-animal variability, bioburden reduction, and different harvesting conditions are challenges that need to be considered when scaling up the dECM hydrogel production from the laboratory to the GMP-graded manufacturing scale.[116] When scaling up to a manufacturing-scale batch, a certain number of donors or animals is required to eliminate batch effects; bioburden reduction is a necessary step that alters the properties and quality of the final product. Hence, the final product must

Table 6. Progress toward clinical translation.

Tissue target	Tissue source	*In vitro* studies	Biocompatability/ Biocompatibility/ histological assessment	Functional studies	Clinical trials	Functional outcomes
Myocardium	Porcine myocardium	[95,96]	[97]	[98–100]	[93]	Clinical trial results support the safety and feasibility of transendocardial injection of VentriGel in post-MI patients with LV dysfunction and introduce a new potential treatment for patients with heart failure[93]
	Human placenta	[101]	[101]	[101]	-	Compared to sham-treated animals, hpECM-injected rat hearts displayed a significant reduction in scar volume and normal electrical activity of the surviving tissue[101]
Skeletal muscle	Porcine hindlimb skeletal muscle	[102]	[102]	-	-	Obtained hydrogels were characterized by superior biocompatibility and low immunogenicity[102]
	Human umbilical cord	[103]	[103]	[103]	-	Improved hindlimb tissue vascularization and perfusion[103]
	Porcine dermis	[104]	[104]	-	-	ECM hydrogels were fully infiltrated with CD68+ cells within 3 days of implantation; CD68+ cells continued to populate the hydrogels at all timepoints and remained in the remodeled tissue after the hydrogel had degraded[104]
Tendon	Human tendon	[105]	[105]	[105]	-	Both fetal bovine serum and hydrogel injection in rats led to more cells inside the tendon compared with culturing[105]
Articular cartilage	Porcine articular cartilage	[106]	-	-	-	Human MSCs cultured on hydrogels from shark skull cartilage, as well as pig articular and auricular cartilage ECM, had increased expression of chondrocyte markers and decreased secretion of angiogenic factors VEGF-A and FGF2[106]
Meniscus	Bovine meniscus	[107]	-	-	-	Region-depended increase of collagen type I and type II and aggrecan expressions in the presence of ECM[107]
Liver	Porcine liver	[108]	-	-	-	Immortalized human hepatocytes were encapsulated in the hydrogels and survived for a week[108]
	Porcine and human livers	[109]	-	-	-	Proliferation rates of organoids cultured in liver ECM hydrogels were lower, but the differentiation capacity of the cholangiocyte organoids towards hepatocyte-like cells is not altered by the presence of tissue-specific ECM components[109]

(*Continue...*)

doi: 10.36922/ijb.4343

Table 6. Continue...

Tissue target	Tissue source	*In vitro* studies	Biocompatability/ Biocompatibility/ histological assessment	Functional studies	Clinical trials	Functional outcomes
Lung	Porcine lung	[32]	-	-	-	A 12-h pepsin digestion of pig lung dECM provides an optimal balance between desirable physical ECM hydrogel properties and effects on lung cell behaviors[32]
Brain	Porcine brain	[30,110]	-	-	-	Rheological results revealed stable hydrogel formation, starting from 5 mg/mL hydrogel; hESCs cultured in ECM exhibited gene expression and differentiation outcomes similar to those cultured in Matrigel[30]
	Human umbilical cord	[111]	[111]	-	-	Injection of umbilical cord-ECM hydrogels into a photothrombotic cortical ischemic lesion in rats resulted in *in vivo* gelation and infiltration with host macrophages[111]
Adipose tissue	Human adipose	[112, 113]	[114]	-	-	From histological assessment, the vascularization process in the hydrogels implanted with adipogenic and endothelial pre-differentiated ASCs was faster than observed in the empty hydrogels[114]

Note: Citations in columns indicate studies on dECM hydrogel in: (i) *in vitro* studies only (least translated), (ii) biocompatibility/histological assessment (i.e., hydrogel injected *in vivo*), (iii) functional study (animal model), and (iv) clinical trials. Abbreviations: ASCs, adipose stem cells; B-ECM, brain extracellular matrix hydrogel; ECM, extracellular matrix; FGF-2, fibroblast growth factor 2; hESCs, human embryonic stem cells; hpECM, human placenta extracellular matrix; LivMA, methacrylated liver extracellular matrix hydrogel; LV, left ventricular; mECM, meniscus extracellular matrix; MI, myocardial infarction; MSCs, mesenchymal stem cells; VEGF-A, vascular endothelial growth factor A.

be evaluated for any changes in its material properties. Different harvesting conditions are also a major factor that can result in inferior quality of the final product.

5.1.1. Challenges associated with the source of dECM

A major concern for large-scale dECM manufacturing is the tissue/organ source used for dECM hydrogel preparation. Three main sources should be considered: patient-derived cells, animal tissues/organs, and human tissues/organs.[117] Cell-derived ECM (CD-ECM) contains a complex and organized mixture of macromolecules that can mimic all aspects of the natural tissue microenvironment.[117] Both primary cells and cell lines have been used to produce CD-EDM. MSCs are easily obtained and are usually used to prepare cell-derived ECM[118] or MBVs (extracellular vesicles bound to ECM crucial for regeneration, especially in 3D conditions).[119] An autologous MSC-derived dECM hydrogel would be an ideal product for clinical translation. Stromal cell-derived ECMs are rich in collagens,[118] while endothelial/epithelial CD-ECMs contain laminin-rich basement membrane-like ECMs.[118] CD-ECM can be generated by scaffold-free 2D and 3D cell cultures.[120] For example, a bioink derived from primary human neonatal dermal fibroblast cell sheets is suitable for 3D bioprinting applications; more importantly, CD-ECM-derived hydrogel retains matrix-deposited growth factors, including EGF, bFGF, NGF, PDGF (A, B, C, and D), IGF-1, TGF-β, and VEGF, in contrast to a dECM hydrogel produced by the standard mild acidified pepsin digestion.[121,122] However, a potential limitation of CD-ECM is its inadequate mechanical properties.

Various tissues from different animals have been widely used to create dECM, such as pig bladder and heart,[123] lung,[32] small intestine,[124] liver,[109] bovine tendons,[125] goat kidney,[126] and rat liver and lungs.[127,128] A major source of heterogeneous dECM is pigs, and the use of swine tissue/organs is superior to other animal sources in many aspects, but one should consider the risk of infection with porcine endogenous retrovirus (PERV).[108]

An animal-to-animal variability as well as different harvesting conditions can significantly affect the resulting properties of the final product, i.e., dECM hydrogels. Evenmore, source variability raises a challenge to a reproducible and standardized manufacturing of dECM materials. Hernandez[116] assessed the effect of animal-to-animal variability and different harvesting conditions on properties of the final dECM hydrogels. The properties of the final dECM hydrogels were evaluated by dsDNA and sGAG quantification, SDS-PAGE gel electrophoresis, and quantitative mass spectrometry. In another study, conducted by Di Francesco et al.,[129] to represent animal-to-animal variability, three out of nine

representative decellularized bovine pericardia were used for experiments, and the properties of the resulting dECM hydrogels prepared from pericardia were assessed by SDS-PAGE gel electrophoresis, rheological characterization, scanning electron microscopy (SEM), and additionally, the influence of animal-to-animal variability on cell viability was assessed by MTS assay. They have shown that although there was a difference in protein composition revealed by mass spectrometry between three different batches, all batches showed the same gelation kinetics, rheological properties, surface structure and same effect in inducing cell viability.[129] Tottey et al.[130] studied the effects of pig source tissue different in age upon extracellular matrix scaffold properties. They have found that the structural, mechanical, and compositional properties of small intestinal submucosa - decellularized extracellular matrix (SIS - dECM) were dependent on the animals' age. For instance, strength (peak load per unit width in uniaxial tensile test) and growth factors content of ECM from 3-week-old animals were less than that of ECM harvested from 12, 26, or >52-week-old animals.[130]

For assessing the effects of animal-to-animal variability on dECM hydrogel properties, longissimus dorsi muscles from four different Yorkshire farm pigs were obtained. Throughout the entire process, including tissue preparation, decellularization, lyophilization, milling, and mild acidified pepsin digestion, all animals were kept separated; but to compare the full batch of a material, the four unfiltered dECM powders from each pig were combined. To assess the effects of different harvesting conditions on the properties of the final dECM hydrogel, longissimus dorsi muscles were obtained from Yorkshire pigs from one source, cross-bred pigs from another source, and boneless pork loin chops from a grocery store. Regarding animal-to-animal variability, there were significant changes in dsDNA and the remaining sGAG content (0.12–1.17 ng dsDNA/mg ECM; 9.13–13.74 μg sGAGs/mg ECM), but these differences fall within the expected ranges for dsDNA and sGAGs. SDS-PAGE did not reveal any differences in the band intensity compared between the four animals. The results of quantitative mass spectrometry revealed that the largest fractions of ECM proteins classified by function were consistent across all the animals, but the amount for each protein was different for each animal. Taken together, it can be concluded that there were minimal effects accounted for animal-to-animal variability; the scaling up from the laboratory to the manufacturing scale would require a larger number of animals to decrease the batch-to-batch variability. However, these differences are still important for the laboratory setting, especially concerning reproducibility. Regarding different harvesting conditions, no significant differences in the residual dsDNA content were found between the three different sources. However, the grocery store batch did not exhibit peptide bands at ~80 and ~90 kDa. The quantitative mass spectrometry data also revealed that, for the grocery store material, the fibrillar collagen and other ECM protein percentages were higher in comparison with the other two sources, while the fractions for the basement membrane were lower. These findings indicate the importance of identifying a feasible raw tissue source and performing quality control experiments.[116]

In order to avoid the spread of disease from animals, i.e., associated with the application of xenogenic dECM, human tissues would be the best choice to produce dECM for clinical applications.[131] Human-derived dECM can be obtained from cadavers, diseased or damaged tissues and organs of patients, and tissues from human tissue biobanks.[131,132] Various tissues and organs from the human body have been used to create dECM. For example, the entire heart,[133] cartilage,[134] ovarian tissue,[135] adipose tissue,[136] pancreas,[137] kidney,[138] liver,[109] skin,[139] teeth,[140] and lungs[141] have been successfully decellularized. However, in the case of cadaveric donors, age is uncontrollable, which leads to great variations in different batches, as non-enzymatic tissue crosslinks tend to increase towards age. Therefore, it is not possible to achieve the industrial-scale production of dECM hydrogels from human tissue sources. Moreover, the sources of autologous and allogeneic tissues are extremely limited.

Interestingly, Willemse et al.[108] prepared dECM hydrogels from porcine and human livers and found differences in Young's modulus and G' depending on the species; porcine liver ECM had a higher G' than human liver ECM. Additionally, by measuring the total protein content, they demonstrated that porcine ECM was digested more efficiently than human ECM, which could be associated with the accumulation of age-related damage and/or non-enzymatic crosslinking of ECM molecules in aged human livers.[108]

5.1.2. Challenges associated with sterilization

For bioburden reduction, sterilization treatment is mandatory and can be achieved via several means throughout the process of dECM hydrogel preparation, among which γ-irradiation is the most frequently used. Typical conditions are presented by an approximate dose of 15 kGy and a duration of about 10 h.[34] There are protocols involving two-step sterilization, on stages of the acellular membrane and milled powder.[36] Another approach is tissue treatment in 0.1% peracetic acid (PAA) solution to reduce bioburden.[116,142,143] Several studies employed a decontamination by soaking the tissue sample in PBS supplemented with penicillin – streptomycin throughout all the decellularization process.[144] However, this may be

insufficient if the dECM source is obtained under unsterile conditions.

6. Future prospects

Currently, several challenges need to be addressed to translate dECM hydrogels into manufacturing and clinical practice. Batch-to-batch variability can affect the manufacturing process of dECM hydrogels slightly.[116] The printability of dECM hydrogels depends on the tissue source, the relative concentration of dECM (i.e., the concentration of pepsin-soluble collagen), and manipulations associated with decellularization and acid hydrolysis. For instance, the G' for 1.37 mg/mL oligomeric collagen is 235 Pa, while that of an 8 mg/mL hydrogel liver dECM is 30 kPa.[145] However, its influence on the printability of dECM hydrogels should not be neglected, as dECM hydrogel batches from different animals of the same species can exhibit different rheological and biomechanical properties. There are no available publications regarding this issue; hence, it is a prospective area for extensive research.

To increase the stability and printability of dECM hydrogels, biorthogonal crosslinking agents should be used, or dECM should be chemically modified with the addition of various functional monomers (acrylate, methacrylate, glycidyl methacrylate, etc.). It should be noted that some "popular" crosslinkers are not biorthogonal. For example, crosslinking using EDC and NHS esters affects the glutamate residue in the GFOGER sequence of collagen, which disrupts cell adhesion.[146] At certain concentrations (IC_{50} = 0.166 mM), genipin has a cytotoxic effect.[147] For these reasons, crosslinking using stepwise (thiol-ene) photopolymerization seems more relevant. An alternative to chemical modification may be the FRESH method.

Unlike microextrusion bioprinting, DMD and DLP bioprinting do not have clear viscosity and viscoelastic property requirements, allowing for the use of suspensions with a higher cell density and is characterized by fewer artifacts compared to extrusion. However, the DMD method requires hydrogel modifications, such as the introduction of functional monomers using photoinitiators, preferably with absorption in the near-UV region (e.g., LAP). The cytotoxicity of hydrogels used in the DMD method is determined mainly by the concentration of the photoinitiator, but practically does not depend on the concentration of the photopolymerized hydrogel.[148]

Therefore, the use of liver dECM as a bioink is promising, as liver dECM hydrogels may contain residual growth factors and GAGs, which serve to deposit growth factors and as nucleation sites during gelation. However, since the process of decellularization and preparation of dECM hydrogels is difficult to standardize, studying the composition of dECM hydrogels in connection with their viscoelastic properties and printability is of high interest.[45,83,129]

Based on the discussion above, the following guidelines for generating dECM hydrogel-based products can be established:

(i) Pre-processing: The source of dECM should be carefully considered in relation to—potential endogenous viral load and—the volume of material required. To minimize batch-to-batch variation, multiple samples should be combined. Additionally, proper sterilization and storage protocols must be implemented.

(ii) Processing: The decellularization technique should be tailored to the specific source material used. Non-chemical decellularization methods are preferable to maintain the integrity of the ECM. Modifications to traditional hydrogel preparation techniques should be selected to preserve essential matrix compounds. The choice of crosslinking mechanisms and bioink composition should align with the desired mechanical properties of the final product.

(iii) 3D bioprinting: The type of bioprinting technology employed should be chosen based on the required resolution and volume of the construct. The geometry of the construct must mimic the structural characteristics of liver components, incorporating pores to facilitate cell function and nutrient exchange.

(iv) Quality control: Each batch of dECM-based products must undergo rigorous quality control assessments, including evaluations of mechanical properties, biocompatibility, and sterility. This ensures consistency and reliability across different production runs.

(v) Application: The final application of dECM hydrogel-based products should be clearly defined, considering factors such as the target tissue or organ system, intended therapeutic outcomes, and regulatory requirements. Understanding the specific application will guide design choices, such as bioink formulation and printing parameters, to optimize functionality and integration within the host environment. This application-focused approach ensures that the developed products effectively meet both scientific and clinical needs.

7. Conclusion

The transition of dECM hydrogels from laboratory research to clinical application presents several significant challenges that must be addressed. The inherent batch-

to-batch variability, influenced by factors such as tissue source and processing techniques, underscores the need for standardized protocols to ensure consistent rheological and biomechanical properties across different hydrogel batches. The potential of liver dECM as a bioink, enriched with growth factors and GAGs, highlights its therapeutic promise, yet necessitates further exploration into its composition and functionality. By adhering to guidelines for producing dECM bioinks, it is feasible to pave the way for the successful integration of dECM hydrogels into clinical practices.

Acknowledgments

The research was conducted at the scientific base of the laboratory established within the framework of the Academic Leadership Program "Priority 2030."

Funding

The work was carried out with financial support from the Ministry of Science and Higher Education of the Russian Federation (grant agreement no. 075-15-2024-640; Sechenov University).

Conflict of interest

Peter S. Timashev serves as a guest editor for the journal but was not in any way (directly or indirectly) involved in the editorial and peer-review process conducted for this paper. The other authors declare they have no competing interests.

Author contributions

Conceptualization: Anastasia I. Shpichka, Anastasiia M. Nesterova, Peter S. Timashev, Massoud Vosough

Figures Visualization: Olga A. Smirnova

Writing – original draft: Valentin A. Brumberg, Zahra Heydari, Polina Yu. Bikmulina, Artem A. Pozdnyakov, Darya R. Zimulkina, Frederico David Alencar de Sena Pereira

Writing – review & editing: Anastasia I. Shpichka, Svetlana L. Kotova, Anastasiia M. Nesterova, Peter S. Timashev

Ethics approval and consent to participate

Not applicable.

Consent for publication

Not applicable.

Availability of data

None.

References

1. Kaur S, Kaur I, Rawal P, Tripathi DM, Vasudevan A. Non-matrigel scaffolds for organoid cultures. *Cancer Lett*. 2021;504:58-66. doi: 10.1016/j.canlet.2021.01.025

2. Bustamante-Torres M, Romero-Fierro D, Arcentales-Vera B, Palomino K, Magaña H, Bucio E. Hydrogels classification according to the physical or chemical interactions and as stimuli-sensitive materials. *Gels*. 2021;7(4):182. doi: 10.3390/gels7040182

3. Chaplenko AA, Khorolsky MD, Melnikova EV, Merkulov VA. Current trends in the use of cell therapy in regenerative medicine. *Bio Prod Prev Diag Treat*. 2020;20(2):82–88. doi: 10.30895/2221-996X-2020-20-2-82-88

4. Ruoß M, Vosough M, Königsrainer A, et al. Towards improved hepatocyte cultures: Progress and limitations. *Food Chem Toxicol*. 2020;138:111188. doi: 10.1016/j.fct.2020.111188

5. Heydari Z, Zarkesh I, Ghanian MH, et al. Biofabrication of size-controlled liver microtissues incorporated with ECM-derived microparticles to prolong hepatocyte function. *Bio-des Manuf*. 2021;4:790-805. doi: 10.1007/s42242-021-00137-4

6. Bikmulina P, Kosheleva N, Efremov Yu, et al. Building a tissue: gingiva- and adipose-derived mesenchymal cell spheroids' survivability and functionality after 3D extrusion bioprinting. *Bioprinting*. 2023;32: e00279. doi: 10.1016/j.bprint.2023.e00279.

7. Mirdamadi ES, Kalhori D, Zakeri N, Azarpira N, Solati-Hashjin M. Liver tissue engineering as an emerging alternative for liver disease treatment. *Tissue Eng Part B Rev*. 2020;26(2):145-163. doi: 10.1089/ten.TEB.2019.0233

8. Ergun C, Parmaksiz M, Vurat MT, Elçin AE, Elçin YM. Decellularized liver ECM-based 3D scaffolds: compositional, physical, chemical, rheological, thermal, mechanical, and in vitro biological evaluations. *Int J Biol Macromol*. 2022;200:110-123. doi: 10.1016/j.ijbiomac.2021.12.086

9. Mao Q, Wang Y, Li Y, et al. Fabrication of liver microtissue with liver decellularized extracellular matrix (dECM) bioink by digital light processing (DLP) bioprinting. *Mater Sci Eng C Mater Biol Appl*. 2020;109:110625. doi: 10.1016/j.msec.2020.110625

10. Heydari Z, Najimi M, Mirzaei H, et al. Tissue engineering in liver regenerative medicine: insights into novel translational technologies. *Cells*. 2020;9(2):304. doi: 10.3390/cells9020304

11. Ranucci CS, Kumar A, Batra SP, Moghe PV. Control of hepatocyte function on collagen foams: sizing matrix pores toward selective induction of 2-D and 3-D cellular morphogenesis. *Biomaterials*. 2000;21(8):783-793.

doi: 10.1016/s0142-9612(99)00238-0

12. Kobayashi M, Kadota J, Hashimoto Y, et al. Elastic modulus of ECM hydrogels derived from decellularized tissue affects capillary network formation in endothelial cells. *Int J Mol Sci*. 2020;21(17):6304.
doi: 10.3390/ijms21176304

13. Ishihara S, Kurosawa H, Haga H. Stiffness-modulation of collagen gels by genipin-crosslinking for cell culture. *Gels*. 2023; 9(2):148.
doi: 10.3390/gels9020148

14. Baptista PM, Siddiqui MM, Lozier G, Rodriguez SR, Atala A, Soker S. The use of whole organ decellularization for the generation of a vascularized liver organoid. *Hepatology*. 2011;53(2):604-617.
doi: 10.1002/hep.24067

15. Karamanos NK, Theocharis AD, Piperigkou Z, et al. A guide to the composition and functions of the extracellular matrix. *FEBS J*. 2021;288(24):6850-6912.
doi: 10.1111/febs.15776

16. Hussey GS, Pineda Molina C, Cramer MC, et al. Lipidomics and RNA sequencing reveal a novel subpopulation of nanovesicle within extracellular matrix biomaterials. *Sci Adv*. 2020;6(12):eaay4361.
doi: 10.1126/sciadv.aay4361

17. Arteel GE, Naba A. The liver matrisome - looking beyond collagens. *JHEP Rep*. 2020;2(4):100115.
doi: 10.1016/j.jhepr.2020.100115

18. Rozario T, DeSimone DW. The extracellular matrix in development and morphogenesis: a dynamic view. *Dev Biol*. 2010;341(1):126-140.
doi: 10.1016/j.ydbio.2009.10.026

19. Heydari Z., Pooyan P, Bikmulina P, et al. Mimicking the liver function in micro-patterned units: challenges and perspectives in 3D bioprinting. *Bioprinting*. 2022;27:e00208.
doi: 10.1016/J.BPRINT.2022.E00208

20. Whiteford JR, Arokiasamy S, De Rossi G. Translating the matrix. *Br J Pharmacol*. 2019;176(1):3-4.
doi: 10.1111/bph.14517

21. Kim J, Seki E. Hyaluronan in liver fibrosis: basic mechanisms, clinical implications, and therapeutic targets. *Hepatol Commun*. 2023;7(4):e0083.
doi: 10.1097/HC9.0000000000000083

22. Gudowska M, Cylwik B, Chrostek L. The role of serum hyaluronic acid determination in the diagnosis of liver fibrosis. *Acta Biochim Pol*. 2017;64(3):451-457.
doi: 10.18388/abp.2016_1443

23. Matsuda M, Seki E. The liver fibrosis niche: Novel insights into the interplay between fibrosis-composing mesenchymal cells, immune cells, endothelial cells, and extracellular matrix. *Food Chem Toxicol*. 2020;143:111556.
doi: 10.1016/j.fct.2020.111556

24. Shan L, Wang F, Zhai D, Meng X, Liu J, Lv X. Matrix metalloproteinases induce extracellular matrix degradation through various pathways to alleviate hepatic fibrosis [published correction appears in Biomed Pharmacother. 2023 Jun;162:114632]. *Biomed Pharmacother*. 2023;161:114472.
doi: 10.1016/j.biopha.2023.114472

25. Hintermann E, Christen U. The many roles of cell adhesion molecules in hepatic fibrosis. *Cells*. 2019;8(12):1503.
doi: 10.3390/cells8121503

26. Freytes DO, O'Neill JD, Duan-Arnold Y, Wrona EA, Vunjak-Novakovic G. Natural cardiac extracellular matrix hydrogels for cultivation of human stem cell-derived cardiomyocytes. *Methods Mol Biol*. 2014;1181:69-81.
doi: 10.1007/978-1-4939-1047-2_7

27. Voytik-Harbin SL, Brightman AO. Small intestinal submucosa: a tissue derived extracellular matrix that promotes tissue-specific growth and differentiation of cells in vitro. *Tissue Eng*. 1998;4:157-174.
doi: 10.1089/ten.1998.4.157

28. Uriel S, Huang JJ, Moya ML, et al. The role of adipose protein derived hydrogels in adipogenesis. *Biomaterials*. 2008;29(27):3712-3719.
doi: 10.1016/j.biomaterials.2008.05.028

29. Kao CY, Nguyen HQ, Weng YC. Characterization of Porcine Urinary Bladder Matrix Hydrogels from Sodium Dodecyl Sulfate Decellularization Method. *Polymers (Basel)*. 2020;12(12):3007.
doi: 10.3390/polym12123007

30. Simsa R, Rothenbücher T, Gürbüz H, et al. Brain organoid formation on decellularized porcine brain ECM hydrogels. *PLoS One*. 2021;16(1):e0245685.
doi: 10.1371/journal.pone.0245685

31. Johnson TD, Lin SY, Christman KL. Tailoring material properties of a nanofibrous extracellular matrix derived hydrogel. *Nanotechnology*. 2011;22(49):494015.
doi: 10.1088/0957-4484/22/49/494015

32. Pouliot RA, Young BM, Link PA, et al. Porcine lung-derived extracellular matrix hydrogel properties are dependent on pepsin digestion time. *Tissue Eng Part C Methods*. 2020;26(6):332-346.
doi: 10.1089/ten.TEC.2020.0042

33. Uriel S, Labay E, Francis-Sedlak M, et al. Extraction and assembly of tissue-derived gels for cell culture and tissue engineering. *Tissue Eng Part C Methods*. 2009;15(3):309-321.
doi: 10.1089/ten.tec.2008.0309

34. Giobbe GG, Crowley C, Luni C, et al. Extracellular matrix hydrogel derived from decellularized tissues enables endodermal organoid culture. *Nat Commun*. 2019;10(1):5658.
doi: 10.1038/s41467-019-13605-4

35. Ijima H, Nakamura S, Bual R, Shirakigawa N, Tanoue S. Physical properties of the extracellular matrix of

decellularized porcine liver. *Gels*. 2018;4(2):39.
doi: 10.3390/gels4020039

36. Hsieh DJ, Srinivasan P. Protocols for accelerated production and purification of collagen scaffold and atelocollagen from animal tissues. *Biotechniques*. 2020;69(3):220-225.
doi: 10.2144/btn-2020-0070

37. Hussey GS, Nascari DG, Saldin LT, et al. Ultrasonic cavitation to prepare ECM hydrogels. *Acta Biomater*. 2020;108:77-86.
doi: 10.1016/j.actbio.2020.03.036

38. Hulmes DJS. *Collagen Diversity, Synthesis, and Assembly*. New York: Springer; 2008.
doi: 10.1007/978-0-387-73906-9_2

39. Kadler KE, Hill A, Canty-Laird EG. Collagen fibrillogenesis: fibronectin, integrins, and minor collagens as organizers and nucleators. *Curr Opin Cell Biol*. 2008;20(5):495-501.
doi: 10.1016/j.ceb.2008.06.008

40. Kayabölen A. *Development of Vascularized Adipose Tissue Construct Based on Adipose Tissue Extracellular Matrix and Silk Fibroin*. M.S. - Master of Science, Middle East Technical University; 2015.

41. Stepanovska J, Otahal M, Hanzalek K, Supova M, Matejka R. pH modification of high-concentrated collagen bioinks as a factor affecting cell viability, mechanical properties, and printability. *Gels*. 2021;7(4):252.
doi: 10.3390/gels7040252

42. Riacci L, Sorriento A, Ricotti L. Genipin-based crosslinking of jellyfish collagen 3D hydrogels. *Gels*. 2021;7(4):238.
doi: 10.3390/gels7040238

43. Utami Nike D, Md Fadilah NI, Sallehuddin N, et al. Genipin-crosslinking effects on biomatrix development for cutaneous wound healing: a concise review. *Front Bioeng Biotechnol*. 2022;10:865014.
doi: 10.3389/fbioe.2022.865014

44. Boso D, Carraro E, Maghin E, et al. Porcine decellularized diaphragm hydrogel: a new option for skeletal muscle malformations. *Biomedicines*. 2021;9(7):709.
doi: 10.3390/biomedicines9070709

45. Zhu H, Cai X, Wu L, Gu Z. A facile one-step gelation approach simultaneously combining physical and chemical cross-linking for the preparation of injectable hydrogels. *J Mater Chem B*. 2017;5(17):3145-3153.
doi: 10.1039/c7tb00396j

46. Cécile E, Laurine V, Jean M, Ahmad M, Gilles S. Chemical cross-linking methods for cell encapsulation in hydrogels. *Materials Today Commun*. 2019; 20:100536, ISSN 2352-4928.
doi: 10.1016/j.mtcomm.2019.05.012

47. Fedorovich NE, Oudshoorn MH, van Geemen D, Hennink WE, Alblas J, Dhert WJ. The effect of photopolymerization on stem cells embedded in hydrogels. *Biomaterials*. 2009;30(3):344-353.
doi: 10.1016/j.biomaterials.2008.09.037

48. Rouillard AD, Berglund CM, Lee JY, et al. Methods for photocrosslinking alginate hydrogel scaffolds with high cell viability. *Tissue Eng Part C Methods*. 2011;17(2):173-179.
doi: 10.1089/ten.TEC.2009.0582

49. Roberts JJ, Bryant SJ. Comparison of photopolymerizable thiol-ene PEG and acrylate-based PEG hydrogels for cartilage development. *Biomaterials*. 2013;34(38):9969-9979.
doi: 10.1016/j.biomaterials.2013.09.020

50. Rydholm AE, Bowman CN, Anseth KS. Degradable thiol-acrylate photopolymers: polymerization and degradation behavior of an in situ forming biomaterial. *Biomaterials*. 2005;26(22):4495-4506.
doi: 10.1016/j.biomaterials.2004.11.046

51. Gwon K, Kim E, Tae G. Heparin-hyaluronic acid hydrogel in support of cellular activities of 3D encapsulated adipose derived stem cells. *Acta Biomater*. 2017;49:284-295.
doi: 10.1016/j.actbio.2016.12.001

52. Brew L. *Development of a Crosslinkable Hydrogel Derived from Placental Tissue*. Master of Philosophy thesis, Queensland University of Technology; 2019.

53. Shi J, Yao H, Wang B, et al. Construction of a decellularized multicomponent extracellular matrix interpenetrating network scaffold by gelatin microporous hydrogel 3d cell culture system. *Macromol Rapid Commun*. 2024;45(5):e2300508.
doi: 10.1002/marc.202300508.

54. Crosby CO, Hillsley A, Kumar S, et al. Phototunable interpenetrating polymer network hydrogels to stimulate the vasculogenesis of stem cell-derived endothelial progenitors. *Acta Biomater*. 2021;122:133-144.
doi: 10.1016/j.actbio.2020.12.041

55. Ma X, Qu X, Zhu W, et al. Deterministically patterned biomimetic human iPSC-derived hepatic model via rapid 3D bioprinting. *Proc Natl Acad Sci U S A*. 2016;113(8):2206-2211.
doi: 10.1073/pnas.1524510113

56. Kim Y, Kang K, Jeong J, et al. Three-dimensional (3D) printing of mouse primary hepatocytes to generate 3D hepatic structure. *Ann Surg Treat Res*. 2017;92(2):67-72.
doi: 10.4174/astr.2017.92.2.67

57. Hiller T, Berg J, Elomaa L, et al. Generation of a 3D liver model comprising human extracellular matrix in an alginate/gelatin-based bioink by extrusion bioprinting for infection and transduction studies. *Int J Mol Sci*. 2018;19(10):3129.
doi: 10.3390/ijms19103129

58. Lewis PL, Green RM, Shah RN. 3D-printed gelatin scaffolds of differing pore geometry modulate hepatocyte function and gene expression. *Acta Biomater*. 2018;69:63-70.
doi: 10.1016/j.actbio.2017.12.042

59. Yang H, Sun L, Pang Y, et al. Three-dimensional bioprinted hepatorganoids prolong survival of mice with liver failure. *Gut*. 2021;70(3):567-574.
doi: 10.1136/gutjnl-2019-319960

60. Lewis PL, Yan M, Su J, Shah RN. Directing the growth and alignment of biliary epithelium within extracellular matrix hydrogels. *Acta Biomater*. 2019;85:84-93. doi: 10.1016/j.actbio.2018.12.039

61. Goulart E, de Caires-Junior LC, Telles-Silva KA, et al. 3D bioprinting of liver spheroids derived from human induced pluripotent stem cells sustain liver function and viability in vitro. *Biofabrication*. 2019;12(1):015010. doi: 10.1088/1758-5090/ab4a30

62. Kang HK, Sarsenova M, Kim DH, et al. Establishing a 3D in vitro hepatic model mimicking physiologically relevant to in vivo state. *Cells*. 2021;10(5):1268. doi: 10.3390/cells10051268

63. Grix T, Ruppelt A, Thomas A, et al. Bioprinting perfusion-enabled liver equivalents for advanced organ-on-a-chip applications. *Genes* (Basel). 2018;9(4):176. doi: 10.3390/genes9040176

64. Liu Tsang V, Chen AA, Cho LM, et al. Fabrication of 3D hepatic tissues by additive photopatterning of cellular hydrogels. *FASEB J*. 2007;21(3):790-801. doi: 10.1096/fj.06-7117com

65. Gibert-Ramos A, Sanfeliu-Redondo D, Aristu-Zabalza P, et al. The hepatic sinusoid in chronic liver disease: the optimal milieu for cancer. *Cancers (Basel)*. 2021;13(22):5719. doi: 10.3390/cancers13225719

66. Murphy SV, Atala A. 3D bioprinting of tissues and organs. *Nat Biotechnol*. 2014;32(8):773-785. doi: 10.1038/nbt.2958

67. Saunders RE, Derby B. Inkjet printing biomaterials for tissue engineering: bioprinting. *Int Mater Rev*. 2014;*59*(8):430-448. doi: 10.1179/1743280414Y.0000000040

68. Cui X, Breitenkamp K, Finn MG, Lotz M, D'Lima DD. Direct human cartilage repair using three-dimensional bioprinting technology. *Tissue Eng Part A*. 2012;18(11-12):1304-1312. doi: 10.1089/ten.TEA.2011.0543

69. Matsusaki M, Sakaue K, Kadowaki K, Akashi M. Three-dimensional human tissue chips fabricated by rapid and automatic inkjet cell printing. *Adv Healthc Mater*. 2013;2(4):534-539. doi: 10.1002/adhm.201200299

70. Dababneh AB, Ozbolat IT. Bioprinting technology: a current state-of-the-art review. *J Manuf Sci Eng*. 2014;136(6):061016. doi: 10.1115/1.4028512

71. Jungst T, Smolan W, Schacht K, Scheibel T, Groll J. Strategies and molecular design criteria for 3D printable hydrogels. *Chem Rev*. 2016;116(3):1496-1539. doi: 10.1021/acs.chemrev.5b00303

72. Chua CK, Yeong WY. *Bioprinting: Principles and Applications*. World Scientific Publishing Co Inc; 2014.

73. You S, Li J, Zhu W, Yu C, Mei D, Chen S. Nanoscale 3D printing of hydrogels for cellular tissue engineering. *J Mater Chem B*. 2018;6(15):2187-2197. doi: 10.1039/C8TB00301G

74. Grigoryan B, Paulsen SJ, Corbett DC, et al. Multivascular networks and functional intravascular topologies within biocompatible hydrogels. *Science*. 2019;364(6439): 458-464. doi: 10.1126/science.aav9750

75. Kim MK, Jeong W, Lee SM, Kim JB, Jin S, Kang HW. Decellularized extracellular matrix-based bio-ink with enhanced 3D printability and mechanical properties. *Biofabrication*. 2020;12(2):025003. doi: 10.1088/1758-5090/ab5d80

76. Lee H, Han W, Kim H, et al. Development of liver decellularized extracellular matrix bioink for three-dimensional cell printing-based liver tissue engineering. *Biomacromolecules*. 2017;18(4):1229-1237. doi: 10.1021/acs.biomac.6b01908

77. Skardal A, Devarasetty M, Kang HW, et al. A hydrogel bioink toolkit for mimicking native tissue biochemical and mechanical properties in bioprinted tissue constructs. *Acta Biomater*. 2015;25:24-34. doi: 10.1016/j.actbio.2015.07.030

78. Mazzocchi A, Devarasetty M, Huntwork R, Soker S, Skardal A. Optimization of collagen type I-hyaluronan hybrid bioink for 3D bioprinted liver microenvironments. *Biofabrication*. 2018;11(1):015003. doi: 10.1088/1758-5090/aae543

79. Jeon H, Kang K, Park SA, et al. Generation of multilayered 3D structures of HepG2 cells using a bio-printing technique. *Gut Liver*. 2017;11(1):121-128. doi: 10.5009/gnl16010

80. Lee JW, Choi YJ, Yong WJ, et al. Development of a 3D cell printed construct considering angiogenesis for liver tissue engineering. *Biofabrication*. 2016;8(1):015007. doi: 10.1088/1758-5090/8/1/015007

81. Bernal PN, Delrot P, Loterie D, et al. Volumetric bioprinting of complex living-tissue constructs within seconds. *Adv Mater*. 2019;31(42):e1904209. doi: 10.1002/adma.201904209

82. Leva V, Chatzipetrou M, Alexopoulos L, Tzeranis DS, Zergioti I. Direct laser printing of liver cells on porous collagen scaffolds. *J Laser Micro Nanoeng*. 2018;13(3):234-237. doi: 10.2961/jlmn.2018.03.0015

83. Yu C, Ma X, Zhu W, et al. Scanningless and continuous 3D bioprinting of human tissues with decellularized extracellular matrix. *Biomaterials*. 2019;194:1-13. doi: 10.1016/j.biomaterials.2018.12.009

84. Antoshin AA, Churbanov SN, Minaev NV, et al. LIFT-bioprinting, is it worth it? *Bioprinting*. 2019;15,2019, doi: 10.1016/j.bprint.2019.e00052.

85. Antoshin A, Minaeva E, Koteneva P, et al. LIFT of cell spheroids: proof of concept. *Bioprinting*. 2023;34: e00297. doi: 10.1016/j.bprint.2023.e00297.

86. Catros S, Fricain JC, Guillotin B, et al. Laser-assisted bioprinting for creating on-demand patterns of human osteoprogenitor cells and nano-hydroxyapatite. *Biofabrication*. 2011;3(2):025001. doi: 10.1088/1758-5082/3/2/025001

87. Koch L, Deiwick A, Schlie S, et al. Skin tissue generation by laser cell printing. *Biotechnol Bioeng*. 2012;109(7):1855-1863. doi: 10.1002/bit.24455

88. Miri AK, Mirzaee I, Hassan S, et al. Effective bioprinting resolution in tissue model fabrication. *Lab Chip*. 2019;19(11):2019-2037. doi: 10.1039/c8lc01037d

89. Ma X, Yu C, Wang P, et al. Rapid 3D bioprinting of decellularized extracellular matrix with regionally varied mechanical properties and biomimetic microarchitecture. *Biomaterials*. 2018;185:310-321. doi: 10.1016/j.biomaterials.2018.09.026

90. Zhu W, Qu X, Zhu J, et al. Direct 3D bioprinting of prevascularized tissue constructs with complex microarchitecture. *Biomaterials*. 2017;124:106-115. doi: 10.1016/j.biomaterials.2017.01.042

91. Zhang X, Zhang X, Li Y, Zhang Y. Applications of light-bBased 3D bioprinting and photoactive biomaterials for tissue engineering. *Materials (Basel)*. 2023;16(23):7461. doi: 10.3390/ma16237461

92. Ovsianikov A, Mühleder S, Torgersen J, et al. Laser photofabrication of cell-containing hydrogel constructs. *Langmuir*. 2014;30(13):3787-3794. doi: 10.1021/la402346z

93. Traverse JH, Henry TD, Dib N, et al. First-in-man study of a cardiac extracellular matrix hydrogel in early and late myocardial infarction patients. *JACC Basic Transl Sci*. 2019;4(6):659-669. doi: 10.1016/j.jacbts.2019.07.012

94. Cai D, Weng W. Development potential of extracellular matrix hydrogels as hemostatic materials. *Front Bioeng Biotechnol*. 2023;11:1187474. doi: 10.3389/fbioe.2023.1187474

95. Fong AH, Romero-López M, Heylman CM, et al. Three-dimensional adult cardiac extracellular matrix promotes maturation of human induced pluripotent stem cell-derived cardiomyocytes. *Tissue Eng Part A*. 2016;22(15-16):1016-1025. doi: 10.1089/ten

96. Gaetani R, Yin C, Srikumar N, et al. Cardiac-derived extracellular matrix enhances cardiogenic properties of human cardiac progenitor cells. *Cell Transplant*. 2016;25(9):1653-1663. doi: 10.3727/096368915X689794

97. Wang RM, Johnson TD, He J, et al. Humanized mouse model for assessing the human immune response to xenogeneic and allogeneic decellularized biomaterials. *Biomaterials*. 2017;129:98-110. doi: 10.1016/j.biomaterials.2017.03.016

98. Pok S, Stupin IV, Tsao C, et al. Full-thickness heart repair with an engineered multilayered myocardial patch in rat model. *Adv Healthc Mater*. 2017;6(5):10.1002/adhm.201600549. doi: 10.1002/adhm.201600549

99. Efraim Y, Sarig H, Cohen Anavy N, et al. Biohybrid cardiac ECM-based hydrogels improve long term cardiac function post myocardial infarction. *Acta Biomater*. 2017;50:220-233. doi: 10.1016/j.actbio.2016.12.015

100. Jang J, Park HJ, Kim SW, et al. 3D printed complex tissue construct using stem cell-laden decellularized extracellular matrix bioinks for cardiac repair. *Biomaterials*. 2017;112:264-274. doi: 10.1016/j.biomaterials.2016.10.026

101. Francis MP, Breathwaite E, Bulysheva AA, et al. Human placenta hydrogel reduces scarring in a rat model of cardiac ischemia and enhances cardiomyocyte and stem cell cultures. *Acta Biomater*. 2017;52:92-104. doi: 10.1016/j.actbio.2016.12.027

102. Barajaa MA, Otsuka T, Ghosh D, Kan HM, Laurencin CT. Development of porcine skeletal muscle extracellular matrix-derived hydrogels with improved properties and low immunogenicity. *Proc Natl Acad Sci USA*. 2024;121(19):e2322822121. doi: 10.1073/pnas.2322822121

103. Ungerleider JL, Johnson TD, Hernandez MJ, et al. Extracellular matrix hydrogel promotes tissue remodeling, arteriogenesis, and perfusion in a rat hindlimb ischemia Model. *JACC Basic Transl Sci*. 2016;1(1-2):32-44. doi: 10.1016/j.jacbts.2016.01.009

104. Wolf MT, Daly KA, Brennan-Pierce EP, et al. A hydrogel derived from decellularized dermal extracellular matrix. *Biomaterials*. 2012;33(29):7028-7038. doi: 10.1016/j.biomaterials.2012.06.051

105. Long C, Galvez MG, Legrand A, et al. Intratendinous injection of hydrogel for reseeding decellularized human flexor tendons. *Plast Reconstr Surg*. 2017;139(6):1305e-1314e. doi: 10.1097/PRS.0000000000003359

106. Burnsed OA, Schwartz Z, Marchand KO, Hyzy SL, Olivares-Navarrete R, Boyan BD. Hydrogels derived from cartilage matrices promote induction of human mesenchymal stem cell chondrogenic differentiation. *Acta Biomater*. 2016;43:139-149. doi: 10.1016/j.actbio.2016.07.034

107. Shimomura K, Rothrauff BB, Tuan RS. Region-specific effect of the decellularized meniscus extracellular matrix on mesenchymal stem cell-based meniscus tissue engineering. *Am J Sports Med*. 2017;45(3):604-611. doi: 10.1177/0363546516674184

108. Ravichandran A, Murekatete B, Moedder D., et al. Photocrosslinkable liver extracellular matrix hydrogels for the generation of 3D liver microenvironment models. *Sci Rep*. 2021;11:15566. doi: 10.1038/s41598-021-94990-z

109. Willemse J, van Tienderen G, van Hengel E, et al. Hydrogels derived from decellularized liver tissue support the growth and differentiation of cholangiocyte organoids. *Biomaterials*. 2022;284:121473.
doi: 10.1016/j.biomaterials.2022.121473

110. Faust A, Kandakatla A, van der Merwe Y, et al. Urinary bladder extracellular matrix hydrogels and matrix-bound vesicles differentially regulate central nervous system neuron viability and axon growth and branching. *J Biomater Appl*. 2017;31(9):1277-1295.
doi: 10.1177/088532821769806

111. Kočí Z, Výborný K, Dubišová J, et al. Extracellular matrix hydrogel derived from human umbilical cord as a scaffold for neural tissue repair and its comparison with extracellular matrix from porcine tissues. *Tissue Eng Part C Methods*. 2017;23(6):333-345.
doi: 10.1089/ten.TEC.2017.0089

112. van Dongen JA, Getova V, Brouwer LA, et al. Adipose tissue-derived extracellular matrix hydrogels as a release platform for secreted paracrine factors. *J Tissue Eng Regen Med*. 2019;13(6):973-985.
doi: 10.1002/term.2843

113. Mahoney CM, Kelmindi-Doko A, Snowden MJ, Peter Rubin J, Marra KG. Adipose derived delivery vehicle for encapsulated adipogenic factors. *Acta Biomater*. 2017;58:26-33.
doi: 10.1016/j.actbio.2017.05.046

114. Kayabolen A, Keskin D, Aykan A, Karslıoglu Y, Zor F, Tezcaner A. Native extracellular matrix/fibroin hydrogels for adipose tissue engineering with enhanced vascularization. *Biomed Mater*. 2017;12(3):035007.
doi: 10.1088/1748-605X/aa6a63

115. Neishabouri A, Soltani Khaboushan A, Daghigh F, Kajbafzadeh AM, Majidi Zolbin M. Decellularization in tissue engineering and regenerative medicine: evaluation, modification, and application methods. *Front Bioeng Biotechnol*. 2022;10:805299.
doi: 10.3389/fbioe.2022.805299

116. Hernandez MJ. *Translation of an Injectable Decellularized Extracellular Matrix Hydrogel for Promoting Skeletal Muscle Regeneration*. University of California San Diego; 2019.

117. Zhang W, Du A, Liu S, Lv M, Chen S. Research progress in decellularized extracellular matrix-derived hydrogels. *Regen Ther*. 2021;18:88-96.
doi: 10.1016/j.reth.2021.04.002

118. Zhu W, Cao L, Song C, Pang Z, Jiang H, Guo C. Cell-derived decellularized extracellular matrix scaffolds for articular cartilage repair. *Int J Artif Organs*. 2021;44(4):269-281.
doi: 10.1177/0391398820953866

119. Peshkova M, Korneev A, Revokatova D, et al. Four sides to the story: A proteomic comparison of liquid-phase and matrix-bound extracellular vesicles in 2D and 3D cell cultures. *Proteomics*. 2024;24(18):e2300375.
doi: 10.1002/pmic.202300375

120. Assunção M, Dehghan-Baniani D, Yiu CHK, Später T, Beyer S, Blocki A. Cell-derived extracellular matrix for tissue engineering and regenerative medicine. *Front Bioeng Biotechnol*. 2020;8:602009.
doi: 10.3389/fbioe.2020.602009

121. Sharma D, Ferguson M, Zhao F. A step-by-step protocol for generating human fibroblast cell-derived completely biological extracellular matrix scaffolds. *Methods Cell Biol*. 2020;156:3-13.
doi: 10.1016/bs.mcb.2019.10.010

122. Lee JS, Nah H, Lee D, et al. Immediately implantable extracellular matrix-enriched osteoinductive hydrogel-laden 3D-printed scaffold for promoting vascularized bone regeneration in vivo. *Mater Des Vol*. 2022; 219:110801.
doi: 10.1016/j.matdes.2022.110801

123. Shin YJ, Shafranek RT, Tsui JH, Walcott J, Nelson A, Kim DH. 3D bioprinting of mechanically tuned bioinks derived from cardiac decellularized extracellular matrix. *Acta Biomater*. 2021;119:75-88.
doi: 10.1016/j.actbio.2020.11.006

124. Casarin M, Fortunato TM, Imran S, et al. Porcine small intestinal submucosa (SIS) as a Suitable Scaffold for the creation of a tissue-engineered urinary conduit: decellularization, biomechanical and biocompatibility characterization using new approaches. *Int J Mol Sci*. 2022;23(5):2826.
doi: 10.3390/ijms23052826

125. Toprakhisar B, Nadernezhad A, Bakirci E, Khani N, Skvortsov GA, Koc B. Development of bioink from decellularized tendon extracellular matrix for 3D bioprinting. *Macromol Biosci*. 2018;18(10):e1800024.
doi: 10.1002/mabi.201800024

126. Vishwakarma SK, Bhavani PG, Bardia A, et al. Preparation of natural three-dimensional goat kidney scaffold for the development of bioartificial organ. *Indian J Nephrol*. 2014;24(6):372-375.
doi: 10.4103/0971-4065.133008

127. Geerts S, Ozer S, Jaramillo M, Yarmush ML, Uygun BE. Nondestructive methods for monitoring cell removal during rat liver decellularization. *Tissue Eng Part C Methods*. 2016;22(7):671-678.
doi: 10.1089/ten.TEC.2015.0571

128. Ren X, Moser PT, Gilpin SE, et al. Engineering pulmonary vasculature in decellularized rat and human lungs. *Nat Biotechnol*. 2015;33(10):1097-1102.
doi: 10.1038/nbt.3354

129. Di Francesco D, Marcello E, Casarella S, et al. Characterization of a decellularized pericardium extracellular matrix hydrogel for regenerative medicine: insights on animal-to-animal variability. *Front Bioeng Biotechnol*. 2024;12:1452965.
doi: 10.3389/fbioe.2024.1452965

130. Tottey S, Johnson SA, Crapo PM, et al. The effect of source animal age upon extracellular matrix scaffold properties. *Biomaterials*. 2011;32(1):128-136.

doi: 10.1016/j.biomaterials.2010.09.006

131. Porzionato A, Stocco E, Barbon S, Grandi F, Macchi V, De Caro R. Tissue-engineered grafts from human decellularized extracellular matrices: a systematic review and future perspectives. *Int J Mol Sci*. 2018;19(12):4117. doi: 10.3390/ijms19124117

132. Meran L, Massie I, Campinoti S, et al. Engineering transplantable jejunal mucosal grafts using patient-derived organoids from children with intestinal failure. *Nat Med*. 2020;26(10):1593-1601. doi: 10.1038/s41591-020-1024-z

133. Garreta E, de Oñate L, Fernández-Santos ME, et al. Myocardial commitment from human pluripotent stem cells: rapid production of human heart grafts. *Biomaterials*. 2016;98:64-78. doi: 10.1016/j.biomaterials.2016.04.003

134. Chen Y, Chen J, Zhang Z, et al. Current advances in the development of natural meniscus scaffolds: innovative approaches to decellularization and recellularization. *Cell Tissue Res*. 2017;370(1):41-52. doi: 10.1007/s00441-017-2605-0

135. Hassanpour A, Talaei-Khozani T, Kargar-Abarghouei E, Razban V, Vojdani Z. Decellularized human ovarian scaffold based on a sodium lauryl ester sulfate (SLES)-treated protocol, as a natural three-dimensional scaffold for construction of bioengineered ovaries. *Stem Cell Res Ther*. 2018;9(1):252. doi: 10.1186/s13287-018-0971-5

136. Brown CF, Yan J, Han TT, Marecak DM, Amsden BG, Flynn LE. Effect of decellularized adipose tissue particle size and cell density on adipose-derived stem cell proliferation and adipogenic differentiation in composite methacrylated chondroitin sulphate hydrogels. *Biomed Mater*. 2015;10(4):045010. doi: 10.1088/1748-6041/10/4/045010

137. Tremmel DM, Sackett SD, Feeney AK, et al. A human pancreatic ECM hydrogel optimized for 3-D modeling of the islet microenvironment. *Sci Rep*. 2022;12(1):7188. doi: 10.1038/s41598-022-11085-z

138. Peloso A, Petrosyan A, Da Sacco S, et al. Renal extracellular matrix scaffolds from discarded kidneys maintain glomerular morphometry and vascular resilience and retains critical growth factors. *Transplantation*. 2015;99(9):1807-1816. doi: 10.1097/TP.0000000000000811.

139. Milan PB, Lotfibakhshaiesh N, Joghataie MT, et al. Accelerated wound healing in a diabetic rat model using decellularized dermal matrix and human umbilical cord perivascular cells. *Acta Biomater*. 2016;45:234-246. doi: 10.1016/j.actbio.2016.08.053

140. Matoug-Elwerfelli M, Duggal MS, Nazzal H, Esteves F, Raïf E. A biocompatible decellularized pulp scaffold for regenerative endodontics. *Int Endod J*. 2018;51(6):663-673. doi: 10.1111/iej.12882

141. Nichols JE, La Francesca S, Vega SP, et al. Giving new life to old lungs: methods to produce and assess whole human paediatric bioengineered lungs. *J Tissue Eng Regen Med*. 2017;11(7):2136-2152. doi: 10.1002/term.2113

142. Yamanaka H, Morimoto N, Yamaoka T. Decellularization of submillimeter-diameter vascular scaffolds using peracetic acid. *J Artif Organs*. 2020;23(2):156-162. doi: 10.1007/s10047-019-01152-0

143. Jiwangga D, Mahyudin F, Mastutik G, Juliana, Meitavany EN. Current Strategies for Tracheal Decellularization: A Systematic Review. *Int J Biomater.* 2024;2024:3355239. doi: 10.1155/2024/3355239

144. Sackett SD, Tremmel DM, Ma F, et al. Extracellular matrix scaffold and hydrogel derived from decellularized and delipidized human pancreas. *Sci Rep*. 2018;8:10452. doi: 10.1038/s41598-018-28857-1

145. Pankajakshan D, Voytik-Harbin SL, Nör JE, Bottino MC. Injectable highly tunable oligomeric collagen matrices for dental tissue regeneration. *ACS Appl Bio Mater*. 2020;3(2):859-868. doi: 10.1021/acsabm.9b00944

146. Kojima H, Kushige H, Yagi H, et al. Combinational treatment involving decellularized extracellular matrix hydrogels with mesenchymal stem cells increased the efficacy of cell therapy in pancreatitis. *Cell Transplant*. 2023;32:9636897231170437. doi: 10.1177/09636897231170437

147. Davidenko N, Schuster CF, Bax DV, et al. Control of crosslinking for tailoring collagen-based scaffolds stability and mechanics. *Acta Biomater*. 2015;25:131-142. doi: 10.1016/j.actbio.2015.07.034

148. Shie MY, Lee JJ, Ho CC, Yen SY, Ng HY, Chen YW. Effects of gelatin methacrylate bio-ink concentration on mechano-physical properties and human dermal fibroblast behavior. *Polymers (Basel)*. 2020;12(9):1930. doi: 10.3390/polym12091930

149. Singh RK, Seliktar D, Putnam AJ. Capillary morphogenesis in PEG-collagen hydrogels. Biomaterials. 2013;34(37):9331-9340. doi: 10.1016/j.biomaterials.2013.08.016

150. Antebi B, Zhang Z, Wang Y, Lu Z, Chen XD, Ling J. Stromal-cell-derived extracellular matrix promotes the proliferation and retains the osteogenic differentiation capacity of mesenchymal stem cells on three-dimensional scaffolds. *Tissue Eng Part C Methods*. 2015;21(2):171-181. doi: 10.1089/ten.TEC.2014.0092

151. Madrid-Wolff J, Boniface A, Loterie D, Delrot P, Moser C. Controlling light in scattering materials for volumetric additive manufacturing. *Adv Sci (Weinh)*. 2022;9(22):e2105144. doi: 10.1002/advs.202105144